Biological Sciences/Microbiology

The *Pseudomonas aeruginosa* T6SS-VgrG1b spike is topped by a PAAR protein eliciting DNA damage to bacterial competitors

Panayiota Pissaridou[a,1], Luke P. Allsopp[a,1], Sarah Wettstadt[a], Sophie A. Howard[a], Despoina A.I. Mavridou[a] and Alain Filloux[a,2]

[a]Imperial College London, Department of Life Sciences, MRC Centre for Molecular Microbiology and Infection, South Kensington Campus, Flowers Building, SW7 2AZ London, United Kingdom.

[1]These authors contributed equally to this work

[2]To whom correspondence should be addressed. A. Filloux, Imperial College London, Department of Life Sciences, MRC Centre for Molecular Microbiology and Infection, South Kensington Campus, Flowers Building, SW7 2AZ London, United Kingdom. Tel.: + 44 (0)2075949651; Fax: + 44 (0)2075943069; E-mail: a.filloux@imperial.ac.uk

AUTHOR CONTRIBUTIONS: P.P., L.P.A and S.A.H. performed research; P.P., S.W., L.P.A., D.A.I.M. and A.F. designed research and analyzed data; P.P., L.P.A, D.A.I.M and A.F. wrote the paper

SHORT TITLE: Tse7 is a T6SS-dependent nuclease

ABSTRACT

The type VI secretion system (T6SS) is a supramolecular complex involved in the delivery of potent toxins during bacterial competition. *Pseudomonas aeruginosa* possesses three T6SS gene clusters and several *hcp* and *vgrG* gene islands, the latter encoding the spike at the T6SS tip. The *vgrG1b* cluster encompasses seven genes whose organization and sequences are highly conserved in *P. aeruginosa* genomes, except for two genes that we called *tse7* and *tsi7*. We show that Tse7 is a Tox-GHH2-domain nuclease which is distinct from other T6SS nucleases identified thus far. Expression of this toxin induces the SOS response, causes growth arrest and ultimately results in DNA degradation. The cytotoxic domain of Tse7 lies at its C-terminus, while the N-terminus is a predicted PAAR domain. We find that Tse7 sits on the tip of the VgrG1b spike and that specific residues at the PAAR - VgrG1b interface are essential for VgrG1b-dependent delivery of Tse7 into bacterial prey. We also show that the delivery of Tse7 is dependent on the H1-T6SS cluster, and injection of the nuclease into bacterial competitors is deployed for inter-bacterial competition. Tsi7, the cognate immunity protein, protects the producer from the deleterious effect of Tse7 through a direct protein-protein interaction so specific that toxin-immunity pairs are effective only if they originate from the same *P. aeruginosa* isolate. Overall, our study highlights the diversity of T6SS effectors, the exquisite fitting of toxins on the tip of the T6SS, and the specificity in Tsi7-dependent protection, suggesting a role in inter-strain competition.

KEYWORDS: T6SS; protein secretion; bacterial toxin; nuclease; PAAR

SIGNIFICANCE STATEMENT

The type VI secretion system (T6SS) is a molecular weapon used for interbacterial competition. It acts like a crossbow bolt to deliver toxic effectors into target cells. Here we characterize a novel T6SS toxin which we call Tse7. We show that it is a DNase and that its two-domain PAAR-nuclease structure allows coupling to the T6SS VgrG tip via the PAAR domain. Disruption of this interface abrogates toxin delivery and results in the loss of interbacterial killing ability. We identify the corresponding immunity protein, Tsi7, and show it directly interacts with the Tse7 toxin. Finally, as Tse7-Tsi7 sequences vary significantly between *P. aeruginosa* strains, and as Tsi7 protection is strain-specific, we show that this toxin-immunity pair contributes to self- non-self-recognition.

\body

INTRODUCTION

Bacterial interactions, positive and negative, are a major determinant during the shaping of polymicrobial communities (1). In the environment or during host colonization different species aim to use efficiently the scarce resources that are available to them and to protect themselves from predators or the immune system. During this process, bacteria cooperate with neighbors to exchange common goods and fight foes competing for the same nutrients or cheaters that exhaust resources without benefiting the community (2).

Bacteria have evolved multiple strategies to fight and eradicate competitors and predators. One such behavior, often employed by *P. aeruginosa*, is the production of high affinity siderophores, which sequester iron and prevent other organisms benefiting from it (3). Another common competitive strategy is the release of diffusible molecules, hydrogen cyanide (4) and pyocyanin (5) by *P. aeruginosa*, or bacteriocins (diffusible toxins) by species like *Escherichia coli* (6). In addition to diffusible toxins, *E. coli* can kill its competitors through systems like the "Contact Dependent Inhibition" (CDI) system (7). In this case, the surface exposed type V secretion system (T5SS) toxin is delivered in a contact-dependent manner into neighboring cells.

The type VI secretion system (T6SS) also results into contact-dependent death or cell stasis (8). It delivers effectors into bacterial cells using a puncturing mechanism similar to that of bacteriophages (9). Functional assembly of the T6SS involves 13-15 core components which form three discrete structures (8). The membrane complex, TssJLM, is the position at which the baseplate docks and through which the puncturing device is engaged. The tail-like structure is made of a contractile sheath, TssBC/VipAB, which encloses a pile of Hcp rings. On top of the Hcp tube sits the puncturing device which consists of a trimer of VgrG proteins

topped by a sharpening PAAR protein (10). Upon contraction of the sheath, its contents are propelled through the membrane complex and into the target cell.

Numerous effectors delivered by the T6SS have been discovered in a broad range of bacteria. Whereas several of these subvert host-cell functions (11), antibacterial toxins are by far the most thoroughly characterized effectors. They have been grouped into families, such as Tae, Tge, Tle or Tde, which stands for type VI amidase, glucosidase, lipase or DNase, effectors, respectively (12, 13). Each antibacterial toxin comes as a pair with a cognate immunity, which protects the bacterium from intoxicating itself or from T6SS-dependent killing by sister cells. T6SS toxins are coupled for transport in various ways, including covalent extensions of Hcp, VgrG or PAAR proteins (termed "evolved"), specific and direct interaction with VgrG or Hcp, or assisted interaction via an adaptor/chaperone with VgrG or PAAR T6SS components (14).

T6SS-dependent bacterial killing was firstly reported in *P. aeruginosa* (15). In this species toxins are often delivered through a mechanism which we previously described as "à la carte delivery" (11), whereby an individual T6SS toxin specifically recognizes its cognate VgrG protein. In such cases, a genetic link (16) can be observed between toxin/immunity pairs and *vgrG* genes. In the present study, we focus on the *vgrG1b* cluster which is genetically associated with the H1-T6SS gene cluster (11, 17). We demonstrate VgrG1b- and H1-T6SS-dependent delivery of a newly-characterized effector which is encoded as a toxin/immunity pair. We show that the toxin, Tse7, is a DNase whose activity is blocked through direct interaction with its cognate immunity Tsi7 protecting the producing cell. The cytotoxic domain of this protein is located at the C-terminus of Tse7, while the N-terminus of the protein forms a PAAR domain which specifically interfaces with the VgrG1b tip. We find toxin/immunity protection to be strain-dependent, suggesting that intra-species competition occurs between *Pseudomonas* strains encoding this cluster, and therefore could be a

contributing factor to the clonal prevalence of *P. aeruginosa* in the lungs of cystic fibrosis patients (18).

RESULTS

The *P. aeruginosa vgrG1b* cluster encodes seven genes. In addition to the three main T6SS clusters in the *P. aeruginosa* genome (H1, H2 and H3), there are orphan clusters that encode components which decorate the tip of the T6SS with a range of toxins (11). One of these clusters carries the *vgrG1b* gene along with six other genes (Fig. 1). Transcriptomic analysis suggests that all seven genes are co-transcribed (19). The *vgrG1b* gene cluster is adjacent to the H1-T6SS cluster (Fig. 1*A*) and co-regulated *via* the Gac/Rsm pathway (20). Bioinformatic analysis of the seven genes (Fig. 1*B*) is summarized in the SI Appendix, Table S1. VgrG1b (PA0095) contains the gp27- and gp5-like hallmarks of all VgrG proteins (21). Based on the conserved features of PA0096, PA0098, PA0099, PA0100 and PA0101 we predict these to encode an OB-fold, a thiolase-like protein, a PAAR protein, a β-propeller protein and a heat-repeat-containing protein, respectively (summarized in SI Appendix, Fig. S1, Table S1). Finally, PA0097 contains a DUF2169 domain, which is thought to have an adaptor/chaperone function allowing some T6SS toxins to be delivered by VgrG proteins (14, 22). Overall, the *vgrG1b* cluster is reminiscent of a nine-gene *vgrG* cluster from *P. mirabilis* termed the *pef* operon which additionally encodes an Hcp protein and a protein of unknown function (Fig. 1*C*) (23).

Tse7 is a putative PAAR-containing nuclease. PA0099, which we call *tse7* (for Type VI secretion effector 7), encodes an N-terminal DUF4150 PAAR-like domain (10) and a C-terminal Tox-GHH2 domain (24) (Fig. 1*B*, SI Appendix, Table S1). Tox-GHH2-containing proteins belong to the HNH nuclease superfamily and have a catalytic-site consensus

S[A/G/P]HH, where the first histidine is responsible for metal ion binding and the second histidine for water hydrolysis. An alignment of Tse7 from *P. aeruginosa* strains shows variability within the C-terminus, including the residues forming the catalytic site (SI Appendix, Fig. S2*A*). Further phylogenetic analysis of Tse7 reveals clear segregation of the *tse7* genes into four clades which is also reflected in differences in the catalytic site sequences (SI Appendix, Fig. S2*AB*).

Tse7 is a bacterial toxin with DNase activity. Tse7 was previously indicated to be toxic (11) and its Tox-GHH2 domain suggests a nuclease activity. To confirm the toxic activity of Tse7, we cloned the *tse7* gene from PAK, $tse7^{PAK}$, in frame with a V5 tag (pTse7) and introduced the recombinant plasmid into *E. coli*. Tse7 expression led to impaired *E. coli* growth (Fig. 2). We engineered a catalytic site mutant with an H183A substitution, $Tse7^{H183A}$, which showed no toxicity when expressed (Fig. 2). This experiment was repeated in the absence of antibiotics and similar results were obtained (SI Appendix, Fig. S3*A*), confirming that *E. coli* death is not due to Tse7-dependent degradation of the plasmid leading to loss of resistance and thus death via antibiotic action. Production of both the wild-type and mutant forms was confirmed by western blot using an anti-V5 antibody (SI Appendix, Fig. S3*B*).

At the early stages of expression of a nuclease toxin, its activity would be expected to cause low levels of DNA damage (for example double-stranded DNA breaks) which would lead to activation of the SOS response (25). To test if Tse7 has such activity, we cloned the promoter region of the *Pseudomonas putida recA* gene upstream of *gfp* in pPROBE-TT′ (p*recA-gfp*), which we used as a DNA-damage reporter. Expression of Tse7, in the presence of this reporter led to significant GFP expression, which was not observed for strains carrying the empty-vector control or encoding the Tse7 catalytic mutant (SI Appendix, Fig. S4*A*). This

Tse7-dependent phenotypic impact could be quantified using flow cytometry (SI Appendix, Fig. S4*BC*, S5*A*); expression of Tse7 resulted in almost half of the cell population producing GFP, as compared to only about 10% in the case of the empty vector or the inactive Tse7 ($Tse7^{H183A}$) (SI Appendix, Fig. S4*D*).

Next, we assessed the enzymatic activity of Tse7 using a DNase assay (12). Expression of Tse7 in *E. coli* from pTse7 led to degradation of the encoding plasmid, which was again not observed for the empty vector or the catalytic site mutant $Tse7^{H183A}$ (Fig. 3*A*). The impact of Tse7 expression was visualized by fluorescence microscopy and resulted in the loss of DAPI-stained DNA in *E. coli* cells (Fig. 3*B*, SI Appendix, Fig. S6). No loss of DAPI staining was observed when cells harbored the empty vector or expressed $Tse7^{H183A}$. Flow cytometry analysis showed that more than 35% of the cells lacked DNA when Tse7 was expressed as compared to approximately 2% of cells harboring the empty vector or expressing $Tse7^{H183A}$ (Fig. 3*CD*, SI Appendix, Fig. S5*B*). To rule out that the loss of DNA from the cells was due to unequal DNA segregation, we performed a DNase assay on radiolabeled exogenous DNA (Fig. 3E). Lysate of *E. coli* expressing Tse7 resulted in degradation of the labeled DNA which was not seen when lysate of *E. coli* expressing $Tse7^{H183A}$ was used. The extent of the degradation is approximately equivalent to what is observed upon addition of DNase I.

Overall, we have confirmed, using several independent methods, that Tse7 is a nuclease toxin with DNase activity which intoxicates *E. coli* and leads to growth arrest.

Tse7 is a VgrG1b-dependent T6SS toxin involved in bacterial competition. Previous studies from our laboratory showed that *P. aeruginosa* compromises the growth of *E. coli* in a VgrG1b-dependent manner (11). We further confirmed this by performing competition assays using *P. putida* as a prey. We use the PAKΔ*retS* strain which is constitutively T6SS

active. In this background, the sole presence of *vgrG1b* is sufficient to mediate killing (Fig. 4*A*), even in the absence of the other H1-T6SS-associated *vgrG* genes, *vgrG1a* and *vgrG1c*. However, in the *vgrG1a/vgrG1c* mutant background, upon deletion of *tse7* or replacement by the gene encoding the Tse7 catalytic mutant (*tse7*^{H183A}), this killing ability is lost (Fig. 4*A*). Therefore, we conclude that Tse7 is injected into target cells in a VgrG1b-dependent manner and exerts toxicity through its nuclease domain. This VgrG1b-dependent delivery is also H1-T6SS-dependent, as killing is lost if the attacker strain is a *tssB1* mutant (H1-T6SS), but not in a *tssB2* mutant (H2-T6SS) (Fig. 4*B*, SI Appendix, Fig. S7*A*).

T6SSs have been shown to be important *in vivo* and during infection (26). To investigate the impact of the *vgrG1b* cluster upon infection progression we employed a *Galleria mellonella* model (27). Infection with a strain deleted for the core H1-T6SS genes resulted in decreased pathogenicity when compared to the wild-type strain (SI Appendix Fig. S8*A*). Furthermore, deleting either *vgrG1b* alone or the entire *vgrG1b* cluster (PA0095-PA0101) also resulted in a reduction in pathogenicity, to the same extent as with the H1-T6SS mutant, suggesting that the *vgrG1b* cluster contributes to virulence in *Galleria mellonella* (SI Appendix, Fig. S8*AB*). However, these observed differences are not exclusively linked with Tse7 as PAKΔ*tse7* did not display a significantly reduced pathogenicity in this model (SI Appendix, Fig. S8*B*).

The Tse7 PAAR domain is required for coupling to the VgrG1b tip. VgrG proteins are key components of the T6SS tip on which toxins can be fitted by direct protein-protein interaction, such as via a PAAR (DUF4150) domain. Tse7 is a putative evolved PAAR T6SS toxin (SI Appendix, Table S1), and using Phyre2 (28) we confirmed that the Tse7-DUF4150 structure has PAAR-like organization (Fig. 5*A*, SI Appendix, Fig. S9). We were able to show direct interaction between VgrG1b (VgrG1b-Flag) and Tse7 (MBP-Tse7) using dot blot

experiments and proved that this interaction is specific (Fig. 5*B*, SI Appendix, Fig. S7*B*). Next, we docked the modeled Tse7 PAAR and VgrG1b structures and could identify residues, T61-I64 and D610-S614, respectively, which are most likely mediating this interaction (Fig. 5*AC*). To test the requirement of this predicted interaction platform, we constructed three-point mutations (T61A, R63Q, I64N) in Tse7 (termed Tse7^{AQN}) and we performed competition assays with attacker strains expressing the wild-type Tse7 or the mutant Tse7^{AQN}. The attacker encoding the mutated Tse7, PAKΔ*retS*Δ*vgrG1ac-tse7*^{AQN}, displayed no killing of *P. putida* and behaved similarly to an attacker strain lacking the *tse7* gene (Fig. 5*D*, SI Appendix, Fig. S7*CD*). We confirmed that both Tse7 and the variant Tse7^{AQN} were biochemically stable when expressed in *E. coli* (SI Appendix, Fig. S7*E*). We conclude that disrupting the interface between Tse7 and VgrG1b abrogates VgrG1b-dependent delivery of Tse7.

Tsi7 is the immunity protein for Tse7 and exhibits strain specificity. Antibacterial T6SS toxins genes are usually encoded alongside a cognate immunity gene. The gene downstream of *tse7*, PA0100 which we now call *tsi7* (Fig. 1), was cloned into pBAD33 (pTsi7). Co-expression of *tsi7* and *tse7* protected DNA from degradation confirming that Tsi7 is the cognate immunity protein of Tse7 (Fig. 6*A*, SI Appendix, Fig. S10*A*). We assessed if protection by the Tsi7 immunity is mediated through direct protein-protein interaction by performing a dot blot experiment using lysates of cells expressing Tsi7 (Tsi7-HA) against several purified proteins (Fig. 6*B*). We observed that Tsi7 interacts with Tse7 (MBP-Tse7) but not with TssB1 (29) or the HA-tagged T3SS effector EspJ (30) confirming a direct and specific Tse7-Tsi7 interaction.

Comparison of the *vgrG1b* gene clusters from four *P. aeruginosa* strains (PAK, PAO1, PA14 and PA7) shows high conservation in sequence across the entire cluster, with

the noticeable exception of the region encoding the Tse7 nuclease domain and Tsi7 (Fig. 6*C*). Tsi7 is a predicted seven-bladed β-propeller protein (SI Appendix, Fig. S11*A*, Table S1) and alignment of Tsi7 sequences from the four *P. aeruginosa* strains shows key variations in sequence in a series of blocks (SI Appendix, Fig. S11*B*). These are not contained in structural elements of the protein and could plausibly be involved in Tsi7-Tse7 interaction (SI Appendix, Fig. S11). To see if protection can be conferred by any Tsi7 protein, the *tsi7* immunity genes from these three strains were cloned and expressed (SI Appendix, Fig. S10*B*). Remarkably, only the cognate PAK Tsi7 ($Tsi7^{PAK}$) could protect against the DNase activity of Tse7 from PAK (Fig. 6*D*). To further validate this result, we performed inter-*P. aeruginosa* competition assays. When PAO1Δ*retS* was used as the attacker it resulted in killing of PAK, however this killing was not significantly different when the prey was the *vgrG1b* cluster mutant (PAKΔPA0095-101) (SI Appendix, Fig. S12). This suggests that Tsi7 from PAK does not protect from Tse7 from PAO1 or that other T6SS toxin/immunity pairs from PAO1 might not exist in PAK. In contrast, PAO1 lacking the *vgrG1b* cluster including *tsi7* (PAO1ΔPA0095-101) was killed by PAO1Δ*retS* significantly more than the WT (SI Appendix, Fig. S12), which confirmed that Tsi7 is needed to protect from PAO1 kin. These results support that specificity exists between the Tse7-Tsi7 toxin-immunity pairs and demonstrate their involvement in inter-*P. aeruginosa* competition.

DISCUSSION

Bacteria frequently use nuclease toxins against their opponents (31), since nucleic acids are central to all living organisms. These nucleases often belong to polymorphic toxin systems (24). Some, like bacteriocins, are released through altruistic cell lysis (6), while others use secretion systems such as the CDI T5SS, the type IV (T4SS), VI (T6SS) and VII (T7SS) secretion systems. Nucleases have either DNase (*e.g.* EsaD (T7SS), $CdiA\text{-}CT_{O11}^{EC869}$

(CDI), colicin E2) or RNase activity (*e.g.* CdiA-CTII^{Bp1026b} (CDI), colicin E6), targeting tRNA or rRNA molecules (6, 7, 12, 32-34). A variety of T6SS nucleases have been identified, including the Toxin_43 domain Tde family from *A. tumefaciens* (12), the colicin/pyocin-related families (*e.g.* Usp, Hcp_ET3/ET4, VPA1263) (35, 36), the endonuclease NS_2 family (*e.g.* RhsA) (33), the Tox-REase1 family (*e.g.* Tke10) (37) and effectors with an HNH endonuclease motif (*e.g.* RhsB, Rhs2, Hcp_ET1, Tke2/4) (33, 35, 37, 38) (SI Appendix, Table S2). Tse7 is the first characterized T6SS Tox-GHH2 member from the HNH family as well as the first T6SS nuclease identified in *P. aeruginosa*. Thus, it adds to the diversity of T6SS effectors in this organism and may explain why *P. aeruginosa* dominates over other microorganisms (39).

Nucleases transported by the T6SS are often extensions of other T6SS proteins. For example, Usp of APEC has a moderately active pyocin/colicin DNase domain and is an evolved Hcp (36). This is also the case for Hcp_ET1 of STEC, which has a C-terminal HNH-DNase domain, and Hcp_ET3 of ETEC with its C-terminal pyocin S3 DNase domain (35). Yet in many instances the T6SS-dependent secretion of these toxins has not been confirmed. Nucleases also come as extensions of Rhs proteins, as is the case with RhsA and RhsB from *D. dadantii* (33) or Tke2 from *P. putida* (37). These Rhs proteins have a N-terminal region containing a PAAR domain (38). Tse7, is similar in this respect as we find it is also fused to a PAAR protein which facilitates its delivery. Note that the DUF4150 domain was first described as PAAR-like (10) while more recently another PAAR-like family (DUF4280) has been identified in the *Francisella tularensis* T6SS effector IglF (40).

In the case of evolved PAAR toxins (11, 41) it is proposed that interaction with a specific VgrG loads the toxin onto the T6SS tip for efficient delivery into prey cells (14, 40). We show that Tse7 can specifically interact with VgrG1b (Fig. 5*B*). Furthermore, the 3D model of the Tse7 PAAR domain fits onto the VgrG1b tip with multiple putative hydrogen bonds

interactions. Mutation of key Tse7 residues in the PAAR-like domain (T61A, R63Q, I64N) prevents delivery of Tse7 into the target cell (Fig. 5*ACD*, SI Appendix, Fig. S7*CD*), which is likely due to the loss of coupling between VgrG1b and Tse7; this is further supporting the "à la carte" concept (11) of specific association between T6SS toxins and a cognate VgrG.

All T6SS antibacterial toxins are encoded as toxin/immunity pairs. Tse7, like the PefD toxin from *P. mirabilis* (23, 42), requires an immunity to protect the producing cell and its sister cells from intoxication (Fig. 6*A*). Tsi7 is similar to the *P. mirabilis* PefE immunity (42). It is a seven-bladed β-propeller protein that blocks the activity of Tse7 through direct protein-protein interaction (Fig. 6*B*). We show that this interaction is highly specific with only the toxin/immunity pair from the same *P. aeruginosa* strain providing protection (Fig. 6*D*). This strict complementarity and the observed variability of the Tse7-Tsi7 pairs between strains suggest a role in competition. We confirmed a role in inter-*Pseudomonas* killing assays with PAO1 surviving attack from PAO1Δ*retS*, which has a constitutively active T6SS, significantly more than PAO1 deleted for the *vgrG1b* cluster containing $tsi7^{PAO1}$. In contrast, PAO1Δ*retS* equally killed PAK or PAKΔPA0095-0101 (*vgrG1b* cluster mutant) which could be explained by the presence of different effectors mediating the killing but could also be because $Tsi7^{PAK}$ is not capable of protecting from $Tse7^{PAO1}$ (SI Appendix, Fig. S12).

Variation in sequences of toxin and immunity pairs but not in other T6SS components has been previously reported between strains of *V. cholerae* (43). In this case diverse effector/immunity modules could be interchangeable for protection during bacterial competition. The idea of self- non-self-recognition is also supported by the function of the *vgrG1b*-like cluster in *P. mirabilis* (*pef* cluster) in the formation of clear demarcations, called Dienes lines, between opposing strain swarms (23, 42). In some cases *P. mirabilis* encodes an additional orphan immunity gene *pef2*, which does not protect from the PefD toxicity (42), but likely provides protection against PefD homologues from related strains. Similarly,

Bacteroides fragilis strains in the human gut microbiota have accumulated multiple immunity genes for toxins that they do not encode to prevent killing by rival strains (44). These findings along with our results on Tsi7 indicate that the evolutionary race for life within a bacterial community does not only depend on the ability to outcompete others but also upon resisting elimination.

In conclusion, in this study we examine the *vgrG1b* cluster and show that it is conserved between *P. aeruginosa* strains, except for the toxin immunity pair, *tse7-tsi7*. We demonstrate that this gene pair encodes a nuclease Tox-GHH2-domain toxin (Tse7) which induces the SOS response and degrades DNA, and a cognate immunity (Tsi7). We find that the latter interacts specifically with the toxin of the same *P. aeruginosa* strain, which makes the action of the *vgrG1b* cluster relevant for inter-strain competition. Finally, we show that coupling of the Tse7 PAAR-like domain to the top of VgrG1b trimer is mediated through specific interactions which are essential for the delivery of Tse7 into prey cells. Ultimately, by characterizing the function, role and delivery of Tse7, we expand on the extraordinary variety of T6SS effectors, and more broadly on the range of *P. aeruginosa* tools for inter-strains and inter-species competition.

MATERIALS AND METHODS

Strains, primers and plasmids are listed in SI Appendix, Tables S3, S4 and S5, respectively. Details for methods, data analysis and associated references are provided in the SI Appendix. Gene deletions, assays for T6SS secretion, western blotting analysis and T6SS killing experiments were performed as previously described (11). Imaging was performed using an Ibidi 35 mm µDish, covered with a 1% agarose pad on an Axio Observer Z1 Fluorescence microscope. For Flow Cytometry the cultures were normalized and incubated for 5 min in PBS+1% Triton X-100, resuspended in PBS and incubated with 100µg/ml DAPI at room

temperature for 1 hour. Cells were analyzed using a FORTESA II (BD Biosciences). Molecular modelling was performed using Phyre2 and PyMOL.

ACKNOWLEDGEMENTS

A.F. is supported by the MRC grants MR/K001930/1 and MR/N023250/1 and the BBSRC grant BB/N002539/1. P.P. and S.A.H. are recipients of PhD studentships from the MRC and S.W. from Imperial College London. L.P.A. is supported by BBSRC grant BB/N002539/1 and a Marie Curie Fellowship (PIIF-GA-2012-328261). D.A.I.M. is funded by the MRC Career Development Award MR/M009505/1. We thank Abderrahman Hachani, Ronan R. McCarthy and Eleni Manoli for training, advice, cloning and protein purification. We thank Dominic J. Pollard and Gad Frankel for providing the purified MBP-EspJ and Jane Srivastava and Jess Rowley from the Department of Life Sciences Flow Cytometry Facility.

REFERENCES

1. Ashby B, Watkins E, Lourenco J, Gupta S, & Foster KR (2017) Competing species leave many potential niches unfilled. *Nat Ecol Evol* 1(10):1495-1501.
2. Rakoff-Nahoum S, Foster KR, & Comstock LE (2016) The evolution of cooperation within the gut microbiota. *Nature* 533(7602):255-259.
3. Purschke FG, Hiller E, Trick I, & Rupp S (2012) Flexible survival strategies of Pseudomonas aeruginosa in biofilms result in increased fitness compared with Candida albicans. *Mol Cell Proteomics* 11(12):1652-1669.
4. Bernier SP, *et al.* (2016) Cyanide Toxicity to Burkholderia cenocepacia Is Modulated by Polymicrobial Communities and Environmental Factors. *Front Microbiol* 7:725.
5. Rada B & Leto TL (2009) Redox warfare between airway epithelial cells and Pseudomonas: dual oxidase versus pyocyanin. *Immunol Res* 43(1-3):198-209.
6. Cascales E, *et al.* (2007) Colicin biology. *Microbiology and molecular biology reviews : MMBR* 71(1):158-229.
7. Willett JL, Ruhe ZC, Goulding CW, Low DA, & Hayes CS (2015) Contact-Dependent Growth Inhibition (CDI) and CdiB/CdiA Two-Partner Secretion Proteins. *J Mol Biol* 427(23):3754-3765.
8. Ho BT, Dong TG, & Mekalanos JJ (2014) A View to a Kill: The Bacterial Type VI Secretion System. *Cell Host Microbe* 15(1):9-21.
9. Leiman PG, *et al.* (2010) Morphogenesis of the T4 tail and tail fibers. *Virol J* 7:355.
10. Shneider MM, *et al.* (2013) PAAR-repeat proteins sharpen and diversify the type VI secretion system spike. *Nature* 500(7462):350-353.
11. Hachani A, Allsopp LP, Oduko Y, & Filloux A (2014) The VgrG proteins are "a la carte" delivery systems for bacterial type VI effectors. *J Biol Chem* 289(25):17872-17884.

12. Ma LS, Hachani A, Lin JS, Filloux A, & Lai EM (2014) Agrobacterium tumefaciens deploys a superfamily of type VI secretion DNase effectors as weapons for interbacterial competition in planta. *Cell Host Microbe* 16(1):94-104.

13. Russell AB, Peterson SB, & Mougous JD (2014) Type VI secretion system effectors: poisons with a purpose. *Nat Rev Microbiol* 12(2):137-148.

14. Cianfanelli FR, *et al.* (2016) VgrG and PAAR Proteins Define Distinct Versions of a Functional Type VI Secretion System. *PLoS Pathog* 12(6):e1005735.

15. Hood RD, *et al.* (2010) A type VI secretion system of Pseudomonas aeruginosa targets a toxin to bacteria. *Cell Host Microbe* 7(1):25-37.

16. Whitney JC, *et al.* (2014) Genetically distinct pathways guide effector export through the type VI secretion system. *Mol Microbiol* 92(3):529-542.

17. Hachani A, *et al.* (2011) Type VI secretion system in Pseudomonas aeruginosa: secretion and multimerization of VgrG proteins. *J Biol Chem* 286(14):12317-12327.

18. van Mansfeld R, *et al.* (2016) Within-Host Evolution of the Dutch High-Prevalent Pseudomonas aeruginosa Clone ST406 during Chronic Colonization of a Patient with Cystic Fibrosis. *PLoS One* 11(6):e0158106.

19. Wurtzel O, *et al.* (2012) The single-nucleotide resolution transcriptome of Pseudomonas aeruginosa grown in body temperature. *PLoS Pathog* 8(9):e1002945.

20. Allsopp LP, *et al.* (2017) RsmA and AmrZ orchestrate the assembly of all three type VI secretion systems in Pseudomonas aeruginosa. *Proc Natl Acad Sci U S A* 114(29):7707-7712.

21. Leiman PG, *et al.* (2009) Type VI secretion apparatus and phage tail-associated protein complexes share a common evolutionary origin. *Proc Natl Acad Sci U S A* 106(11):4154-4159.

22. Bondage DD, Lin JS, Ma LS, Kuo CH, & Lai EM (2016) VgrG C terminus confers the type VI effector transport specificity and is required for binding with PAAR and adaptor-effector complex. *Proc Natl Acad Sci U S A* 113(27):E3931-3940.

23. Alteri CJ, *et al.* (2013) Multicellular bacteria deploy the type VI secretion system to preemptively strike neighboring cells. *PLoS Pathog* 9(9):e1003608.

24. Zhang D, de Souza RF, Anantharaman V, Iyer LM, & Aravind L (2012) Polymorphic toxin systems: Comprehensive characterization of trafficking modes, processing, mechanisms of action, immunity and ecology using comparative genomics. *Biology direct* 7:18.

25. Kreuzer KN (2013) DNA damage responses in prokaryotes: regulating gene expression, modulating growth patterns, and manipulating replication forks. *Cold Spring Harb Perspect Biol* 5(11):a012674.

26. Fu Y, Waldor MK, & Mekalanos JJ (2013) Tn-Seq analysis of vibrio cholerae intestinal colonization reveals a role for T6SS-mediated antibacterial activity in the host. *Cell Host Microbe* 14(6):652-663.

27. Koch G, Nadal-Jimenez P, Cool RH, & Quax WJ (2014) Assessing Pseudomonas virulence with nonmammalian host: Galleria mellonella. *Methods Mol Biol* 1149:681-688.

28. Kelley LA, Mezulis S, Yates CM, Wass MN, & Sternberg MJ (2015) The Phyre2 web portal for protein modeling, prediction and analysis. *Nat Protoc* 10(6):845-858.

29. Lossi NS, *et al.* (2013) The HsiB1C1 (TssB-TssC) complex of the Pseudomonas aeruginosa type VI secretion system forms a bacteriophage tail sheathlike structure. *J Biol Chem* 288(11):7536-7548.

30. Young JC, *et al.* (2014) The Escherichia coli effector EspJ blocks Src kinase activity via amidation and ADP ribosylation. *Nat Commun* 5:5887.

31. Morse RP, *et al.* (2012) Structural basis of toxicity and immunity in contact-dependent growth inhibition (CDI) systems. *Proc Natl Acad Sci U S A* 109(52):21480-21485.

32. Cao Z, Casabona MG, Kneuper H, Chalmers JD, & Palmer T (2016) The type VII secretion system of Staphylococcus aureus secretes a nuclease toxin that targets competitor bacteria. *Nat Microbiol* 2:16183.

33. Koskiniemi S, *et al.* (2013) Rhs proteins from diverse bacteria mediate intercellular competition. *Proc Natl Acad Sci U S A* 110(17):7032-7037.

34. Souza DP, *et al.* (2015) Bacterial killing via a type IV secretion system. *Nat Commun* 6:6453.

35. Ma J, *et al.* (2017) The Hcp proteins fused with diverse extended-toxin domains represent a novel pattern of antibacterial effectors in type VI secretion systems. *Virulence* 8(7):1189-1202.

36. Nipic D, Podlesek Z, Budic M, Crnigoj M, & Zgur-Bertok D (2013) Escherichia coli uropathogenic-specific protein, Usp, is a bacteriocin-like genotoxin. *J Infect Dis* 208(10):1545-1552.

37. Bernal P, Allsopp LP, Filloux A, & Llamas MA (2017) The Pseudomonas putida T6SS is a plant warden against phytopathogens. *ISME J* 11(4):972-987.

38. Alcoforado Diniz J & Coulthurst SJ (2015) Intraspecies Competition in Serratia marcescens Is Mediated by Type VI-Secreted Rhs Effectors and a Conserved Effector-Associated Accessory Protein. *J Bacteriol* 197(14):2350-2360.

39. Basler M, Ho BT, & Mekalanos JJ (2013) Tit-for-tat: type VI secretion system counterattack during bacterial cell-cell interactions. *Cell* 152(4):884-894.

40. Rigard M, *et al.* (2016) Francisella tularensis IglG Belongs to a Novel Family of PAAR-Like T6SS Proteins and Harbors a Unique N-terminal Extension Required for Virulence. *PLoS Pathog* 12(9):e1005821.

41. Whitney JC, *et al.* (2015) An interbacterial NAD(P)(+) glycohydrolase toxin requires elongation factor Tu for delivery to target cells. *Cell* 163(3):607-619.

42. Alteri CJ, *et al.* (2017) Subtle variation within conserved effector operon gene products contributes to T6SS-mediated killing and immunity. *PLoS Pathog* 13(11):e1006729.

43. Unterweger D, *et al.* (2014) The Vibrio cholerae type VI secretion system employs diverse effector modules for intraspecific competition. *Nat Commun* 5:3549.

44. Wexler AG, *et al.* (2016) Human symbionts inject and neutralize antibacterial toxins to persist in the gut. *Proc Natl Acad Sci U S A* 113(13):3639-3644.

45. Sullivan MJ, Petty NK, & Beatson SA (2011) Easyfig: a genome comparison visualizer. *Bioinformatics* 27(7):1009-1010.

456 **FIGURE LEGENDS**

457

458

459 **Fig. 1. The H1-T6SS and *vgrG1b* clusters.** (*A*) Schematic representation of the genomic
460 organization of the H1-T6SS cluster (in light grey) and the *vgrG1b* cluster in *P. aeruginosa*
461 (genes of interest are indicated according to the color key). (*B*) Schematic representation of
462 the *vgrG1b* cluster. The lower panel shows predicted protein domains as described in SI
463 Appendix, Table S1. (*C*) Schematic representation of the *vgrG* cluster of *P. mirabilis*.
464 Similarities to the *vgrG1b* cluster are indicated using the same color coding as in panel (*B*).

465

466 **Fig. 2. Tse7 is toxic to *E. coli*.** (*A*) Growth curves of *E. coli* BL21 pLysS cells harboring
467 pET28a, pTse7 or pTse7^{H183A}. The arrow indicates the time of induction with 0.5 mM IPTG,
468 while (+) and (-) symbols indicate addition or not of IPTG, respectively. Expression of Tse7
469 compromised growth (grey curve) whilst expression of Tse7^{H183A} did not (blue curve).

470

471 **Fig. 3. Tse7 is a DNase toxin.** (*A*) Nuclease assay demonstrating that expression of Tse7 for
472 two hours results in plasmid degradation. Degradation is not observed for the empty vector
473 (pET28a), the catalytic mutant or the uninduced Tse7. (*B*) Expression of Tse7 results in loss
474 of DNA staining (DAPI) from *E. coli* cells. Fluorescence microscopy of *E. coli* cells
475 harboring pET28a, pTse7 or pTse7^{H183A} two hours after IPTG induction and staining with
476 DAPI. Scale bars are at 6 µm. Channel separation can be seen in the SI Appendix, Fig. S5.
477 (*C*) Flow cytometry analysis confirming that expression of Tse7 results in reduction in the
478 number of cells containing DAPI-stained DNA. The *x*-axis, labeled "DAPI", corresponds to
479 450_50V_H filter reading. (*D*) Quantification of (*C*), the graph illustrates n=3 flow cytometry
480 experiments ±SD; two-way ANOVA Sidak's multiple comparisons test (*** equals P ≤

0.001). (*E*) Tse7 degrades exogenous DNA. *E. coli* BL21 lysates harboring the plasmids of interest were co-incubated for 20 min with ^{32}P-labeled PCR product prior to gel analysis and detection. In panels (A) and (E), (+) and (-) indicates addition or not of IPTG, respectively.

Fig. 4. Tse7 is a H1-T6SS toxin dependent on VgrG1b for killing of *P. putida.* (*A*) Quantification of a bacterial competition assay between *P. aeruginosa* and *P. putida*/pRL662-*gfp*. On the *y* axis, the level of fluorescence recorded indicates survival of *P. putida*. PAKΔ*retS* is active for H1-T6SS-dependent killing. Deletion of *vgrG1abc* in the attacker cell (PAKΔ*retS*Δ*vgrG1ac*Δ*vgrG1b*) abrogates killing, however a strain deleted for only *vgrG1ac* (PAKΔ*retS*Δ*vgrG1ac*) still kills. Killing is Tse7-dependent as it is lost if *tse7* is deleted (PAKΔ*retS*Δ*vgrG1ac*Δ*tse7*) or the catalytic site is mutated (PAKΔ*retS*Δ*vgrG1ac*Δ*tse7*^{H183A}). (*B*) Quantification of bacterial competition assays showing that the core H1-T6SS component TssB1 is required for killing, but the H2-T6SS component TssB2 is not. (*A*) and (*B*) are the average of n=3 independent experiments ±SD; statistical significance indicated (**** equals $P \leq 0.0001$) one-way ANOVA Dunnett's multiple comparison test against the first column.

Fig. 5. Tse7 tops the VgrG1b puncturing device to enable bacterial killing. (*A*) Tse7 (red) and VgrG1b trimer (green) modeled structures fitted together, blue color illustrates the three PAAR motifs identified in Tse7 (see also SI Appendix, Fig. S9). (*B*) Dot blots demonstrating direct interaction between Tse7 and VgrG1b. Purified MBP-Tse7 was spotted on the membrane, blocked and then incubated with VgrG1b-Flag-, VgrG2b-Flag- or Hcp1-Flag-containing lysate. The interaction was shown using an anti-Flag antibody. Purified MBP-EspJ was used as a negative control. The presence of the purified protein was confirmed using specific antibodies against MBP. (*C*) Pull out of Tse7 and VgrG1b with the putative interacting residues colored in grey (T61, R63 and I64 for Tse7, D610, T612 and I613 for

VgrG1b). Tse7 residues where mutated (T61A, R63Q, I64N; the variant gene is then termed *tse7*^{AQN}) to assess the interaction at the VgrG1b-Tse7 interface. (*D*) Competition assay showing loss of *P. putida* killing when competing with a *tse7*^{AQN} mutant, as is the case for a *vgrG1b* or *tse7* deletion mutant (see also SI Appendix, Fig. S7*CD*). Results are the average of n=3 independent experiments ±SD; statistical significance indicated (**** equals $P \leq 0.0001$) one-way ANOVA Dunnett's multiple comparison test against the first column.

Fig. 6. Tsi7 is the cognate immunity of Tse7 and exhibits strain specificity. (*A*) Nuclease assay showing that Tsi7 protects cells from the Tse7 DNase activity. (*B*) Dot blots demonstrating direct interaction between Tse7 and Tsi7. Purified MBP-Tse7 was spotted on the membrane, blocked and then incubated with Tsi7-HA lysate. The interaction was shown using an anti-HA antibody (left-hand panel). Purified TssBC1 and MBP-EspJ were used as controls. The presence of the purified proteins was confirmed using antibodies against TssB1 or MBP (right-hand panels). (*C*) Genome sequence alignment of the *vgrG1b* region demonstrating the divergence of the 3´-end of *tse7* and of *tsi7* in four *P. aeruginosa* strains using Easyfig (45). (*D*) Nuclease assay demonstrating strain specificity of Tse7 immunity proteins. Only Tsi7 from PAK, and no other Tsi7 immunity protein, is capable of protecting from Tse7^{PAK}. In panels (A) and (D), (+) and (-) symbols indicate addition or not of IPTG, respectively.

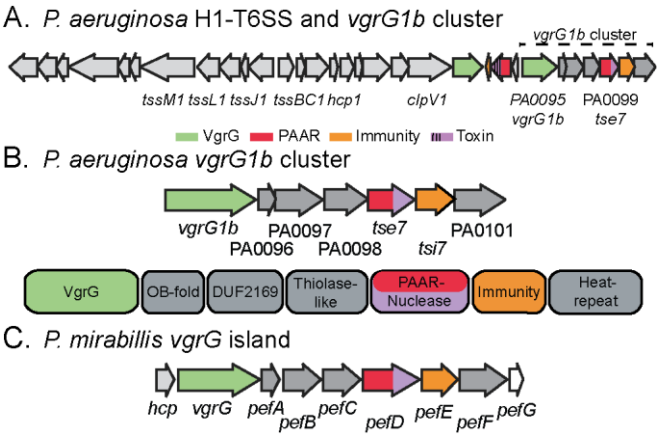
A. P. aeruginosa H1-T6SS and vgrG1b cluster
vgrG1b cluster
tssM1 tssL1 tssJ1 tssBC1 hcp1
clpV1
PA0095
vgrG1b
PA0099
tse7
VgrG
PAAR
Immunity
Toxin
B. P. aeruginosa vgrG1b cluster
vgrG1b
PA0097
PA0096
PA0098
tse7
tsi7
PA0101
VgrG
OB-fold
DUF2169
Thiolase-like
PAAR-Nuclease
Immunity
Heat-repeat
C. P. mirabillis vgrG island
hcp
vgrG
pefA
pefB
pefC
pefD
pefE
pefF
pefG

Figure 1

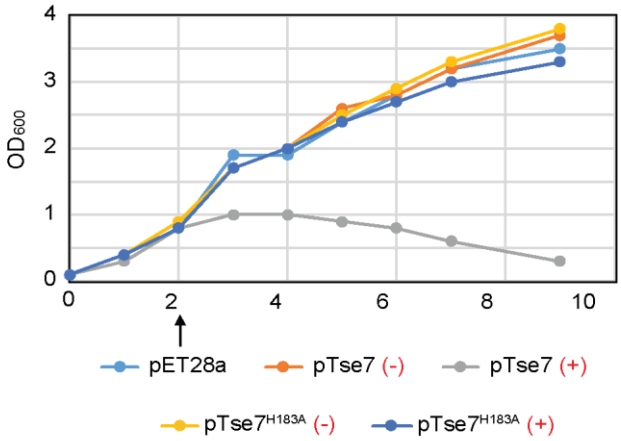
4
3
2
1
0
OD600
0
2
4
6
8
10
pET28a
pTse7 (-)
pTse7 (+)
pTse7H183A (-)
pTse7H183A (+)

Figure 2

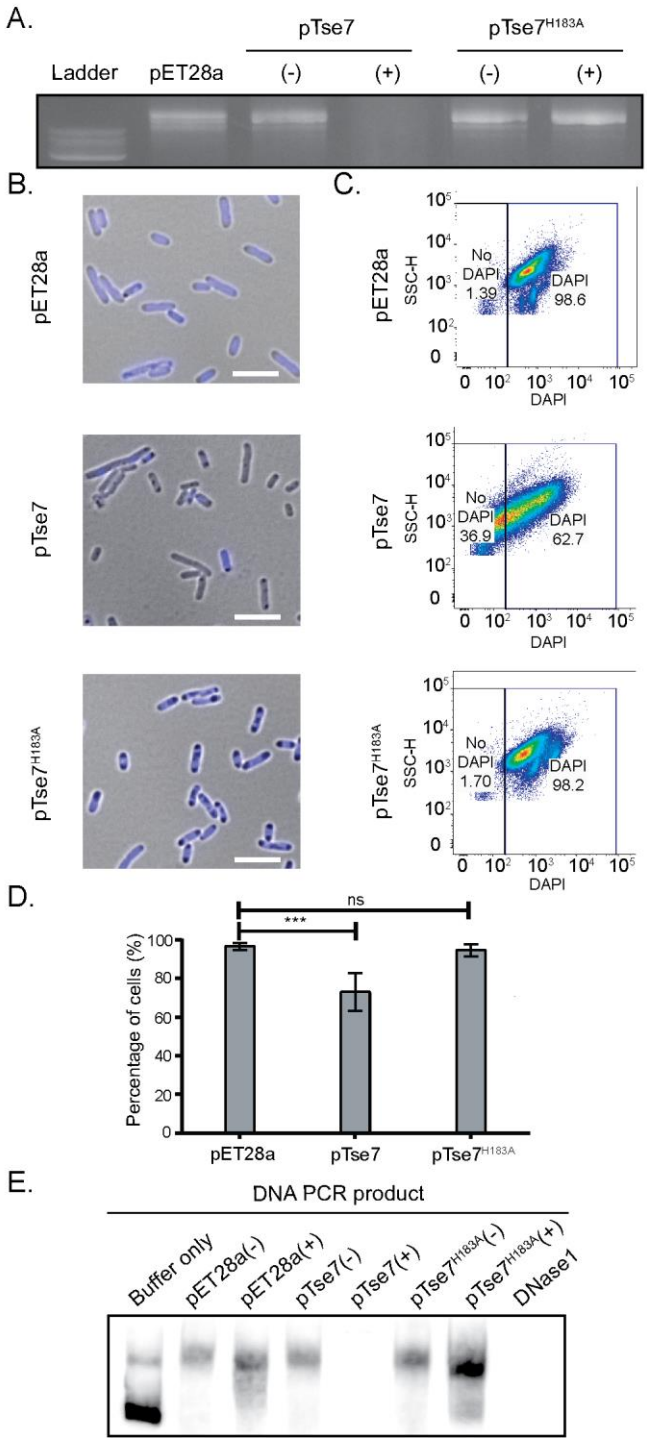
A.
pTse7
pTse7H183A
Ladder
pET28a
(-)
(+)
(-)
(+)
B.
C.
pET28a
pTse7
pTse7H183A
SSC-H
DAPI
No DAPI 1.39
DAPI 98.6
No DAPI 36.9
DAPI 62.7
No DAPI 1.70
DAPI 98.2
D.
ns
***
Percentage of cells (%)
pET28a
pTse7
pTse7H183A
E.
DNA PCR product
Buffer only
pET28a(-)
pET28a(+)
pTse7(-)
pTse7(+)
pTse7H183A(-)
pTse7H183A(+)
DNase1

Figure 3

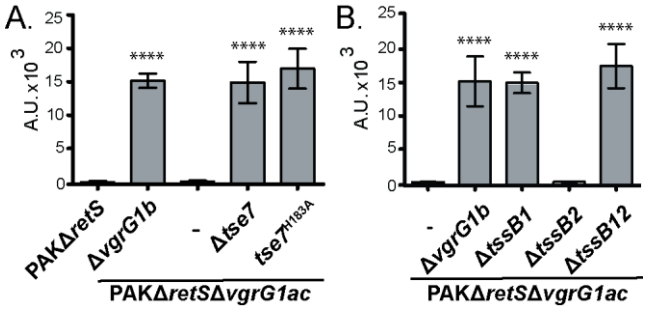
A.
B.
A.U. x10 3
25
20
15
10
5
0
****
PAKΔretS
ΔvgrG1b
-
Δtse7
tse7T183A
PAKΔretSΔvgrG1ac
ΔtssB1
ΔtssB2
ΔtssB12

Figure 4

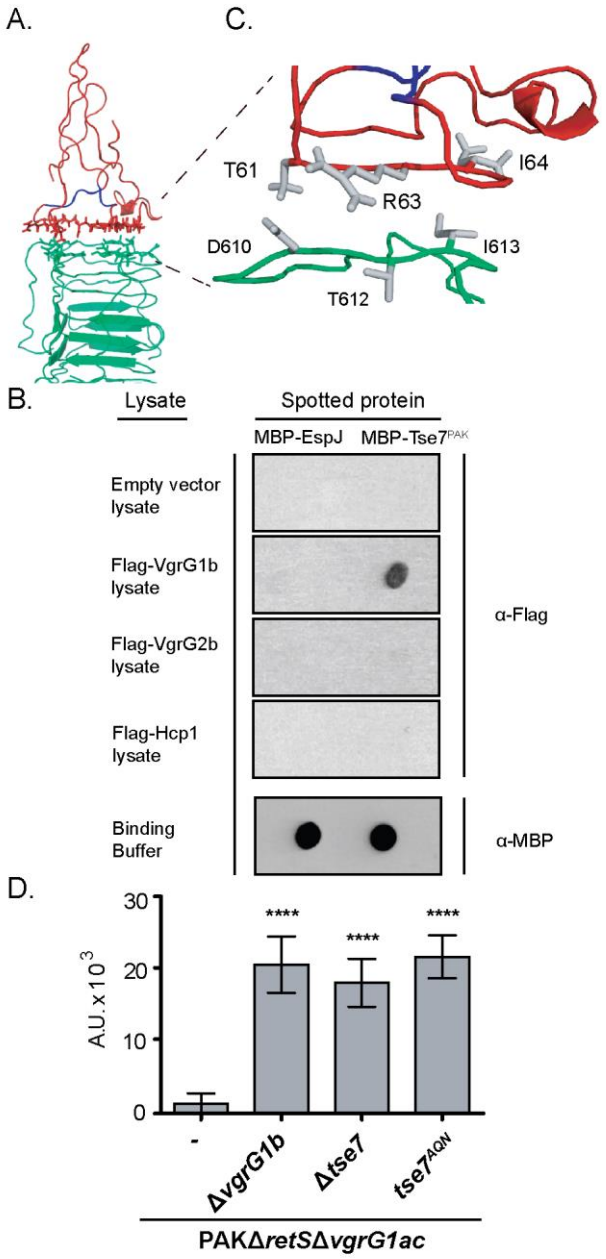
A.
C.
T61
I64
R63
D610
I613
T612
B.
Lysate
Spotted protein
MBP-EspJ
MBP-Tse7PAK
Empty vector lysate
Flag-VgrG1b lysate
Flag-VgrG2b lysate
Flag-Hcp1 lysate
Binding Buffer
α-Flag
α-MBP
D.
A.U. x 10^3
30
20
10
0
****
****
****
-
ΔvgrG1b
Δtse7
tse7AQN
PAKΔretSΔvgrG1ac

Figure 5

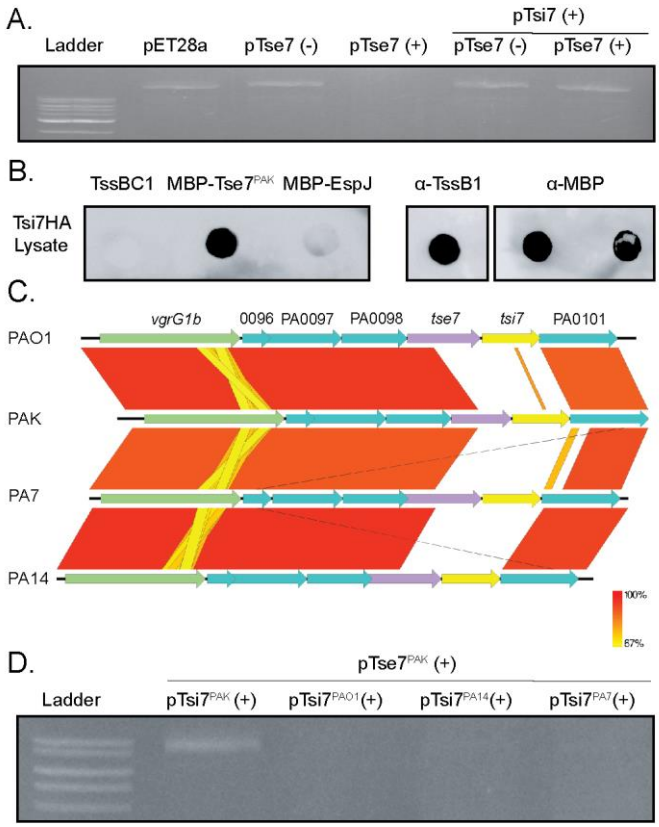
A.
pTsi7 (+)
Ladder
pET28a
pTse7 (-)
pTse7 (+)
pTse7 (-)
pTse7 (+)
B.
TssBC1
MBP-Tse7PAK
MBP-EspJ
α-TssB1
α-MBP
Tsi7HA Lysate
C.
vgrG1b
0096
PA0097
PA0098
tse7
tsi7
PA0101
PAO1
PAK
PA7
PA14
100%
87%
D.
pTse7PAK (+)
Ladder
pTsi7PAK (+)
pTsi7PAO1(+)
pTsi7PA14(+)
pTsi7PA7(+)

Figure 6

SUPPLEMENTARY INFORMATION (SI) APPENDIX FOR

The *Pseudomonas aeruginosa* T6SS-VgrG1b spike is topped by a PAAR protein eliciting DNA damage to bacterial competitors

Panayiota Pissaridou[a,1], Luke P. Allsopp[a,1], Sarah Wettstadt[a], Sophie A. Howard[a], Despoina A.I. Mavridou[a] and Alain Filloux[a,2]

[a]Imperial College London, Department of Life Sciences, MRC Centre for Molecular Microbiology and Infection, South Kensington Campus, Flowers Building, SW7 2AZ London, United Kingdom.

[1]These authors contributed equally to this work

[2]To whom correspondence should be addressed. A. Filloux, Imperial College London, Department of Life Sciences, MRC Centre for Molecular Microbiology and Infection, South Kensington Campus, Flowers Building, SW7 2AZ London, United Kingdom. Tel.: + 44 (0)2075949651; Fax: + 44 (0)2075943069; E-mail: a.filloux@imperial.ac.uk

This PDF file includes:

Supplementary Materials and Methods
Figs. S1 to S12
Tables S1 to S5
References for SI reference citations

SUPPLEMENTARY INFORMATION MATERIALS AND METHODS

Bacterial strains and growth conditions. Bacterial strains are listed in Table S3. *E. coli* strains were grown at 37°C in Lysogeny Broth. *Pseudomonas* strains were grown in Tryptone Soy Broth at 37°C and 30°C for *Pseudomonas aeruginosa* and *Pseudomonas putida* strains, respectively. Antibiotics (Sigma) were supplemented where necessary: for *P. aeruginosa* streptomycin, 2000 µg/ml, gentamicin 50 µg/ml; for *P. putida* mitomycin C 2 µg/ml, rifampicin 20 µg/ml, gentamicin 50 µg/ml; for *E. coli* streptomycin 50 µg/ml, tetracycline 15 µg/ml, ampicillin 50–100 µg/ml, kanamycin 50 µg/ml, chloramphenicol 34 µg/ml, mitomycin C 1 µg/ml and gentamicin 15 µg/ml.

Molecular cloning. Genes and mutator fragments used in this study were amplified with KOD Hot Start DNA Polymerase (Novagen) in the presence of Betaine (Sigma). Primers used are listed in Table S4. Genes or DNA fragments of interest were amplified from *P. aeruginosa* PAK, PAO1, PA7, PA14 or from *P. putida* KT2440. For the pET28a constructs, the *tse7-V5* PCR products were restricted with *Bam*HI and *Xho*I (Roche). For the pBAD33 construct, *tsi7*-HA was restricted using *Xba*I and *Hin*dIII (Roche). The pMALxE constructs were cloned using *Bam*HI and *Xba*I. For the pME6032 constructs, *vgrG1b* (PA0095), *vgrG2b* (PA0262) and *hcp1* (PA0085) were amplified and digested using *Eco*RI, *Nco*I, *Bgl*II or *Sac*I according to the respective primers. pP*recA-gfp* was constructed by amplifying *recA* from *P. putida* KT2440 followed by digestion with *Bam*HI and *Hin*dIII and cloning into pPROBE-TT´. All constructs were ligated using T4 ligase (Roche) and transformed in *E. coli* DH5α. Constructs were confirmed using standard Taq polymerase (New England Biolabs), in the presence of DMSO (Sigma) and according to the manufacturer's instructions. Isolation of plasmid DNA was carried out using the QIAprep spin miniprep kit (Qiagen). All constructs were confirmed via DNA sequencing (GATC Biotech) and are listed in Table S5.

Pseudomonas mutant construction. Deletion of genes of interest was performed as previously described (1). pKNG101 constructs containing a DNA mutator fragment including 500 bp upstream and 500 bp downstream of the gene(s) of interest were generated (see table S4). Plasmids were then conjugated into *P. aeruginosa* strains. The pKNG101 mutators were integrated into the chromosome through homologous recombination and bacteria were selected on streptomycin-containing LB plates (Sm2000). Colonies where a second recombination event, resulting in excision of pKNG101 from the genome, had occurred were selected by streaking the bacteria onto 20% sucrose; pKNG101 encodes the *sacB* gene which when expressed produces a toxic product from sucrose which is lethal to Gram-negative bacteria (2). Sm2000-sensitive clones were analyzed and deletion of the gene of interest confirmed by colony PCR using standard Taq polymerase (New England Biolabs).

Bacterial toxicity assay. Overnight bacterial cultures were used to inoculate 10 ml of media at a starting OD_{600} of 0.1. Flasks were incubated at 37°C and expression of potential toxin genes was induced after 2 hours with 0.5 mM IPTG (Melford) or 0.2% arabinose (Sigma). OD_{600} readings were taken every hour. At 4 hours samples from both induced and non-induced cultures were prepared for western blotting analysis.

DNase assay and Flow Cytometry. Overnight bacterial cultures were diluted into 10 ml cultures to a final OD_{600} 0.1 and gene expression was induced with 0.5 mM IPTG and/or 0.2% arabinose. Cultures were grown at 37°C for 2 hours. Cultures were fixed to an OD_{600} of 1 and plasmid extraction using the Qiagen Miniprep Kit was performed. Resulting extracts were then subjected to electrophoresis on a 1% agarose gel containing SafeView (NBS

Biologicals) and visualized using Quantum. For Flow Cytometry analysis, cultures were normalized and incubated for 5 min in PBS+1% Triton X-100, then resuspended again in PBS and incubated with 100 µg/ml DAPI at room temperature for 1 hour. Cells were then analyzed using a FORTESA II (BD Biosciences).

Radiolabeled DNase assay. Target DNA was the *tssA2* promoter region previously used in (3). This region was amplified with primers *tssA2*_F and *tssA2*_R. Subsequently, 5 pMol of the DNA was labelled with ^{32}P-γATP using T4 Kinase following the manufactures instructions (New England Biolabs). Labeled DNA was purified using a QIAquick PCR purification kit (Qiagen). Eluted DNA was quantified using a Qubit2 Fluorometer. Cultures were grown, and genes induced, where appropriate, as above. Fifteen OD_{600} units were centrifuged and resuspended in 2 ml of DNase I buffer (10 mM Tris-HCl, 2.5 mM $MgCl_2$, 0.5 mM $CaCl_2$ pH 7.6). Samples were then sonicated on ice followed by centrifugation at 4000 RPM for 2 min. In Eppendorf tubes, 9 µl of buffer, 9 µl of lysate, or 8 µl of buffer and 1 µl of DNase I (New England Biolabs) were mixed with 5 nM of ^{32}P-labeled DNA and incubated at 37°C for 20 min. Prior to gel loading, 2 µl of native loading dye was added and the entire sample loaded. Samples were subjected to electrophoresis on 4% (w/v) 0.5% TBE native polyacrylamide gels at 200V for 22 minutes prior to drying. Imaging was performed on a Typhoon FLA7000 Phosphorimager (GE Healthcare).

Bacterial competition assay. Bacterial competitions were carried out as described before (4). Briefly, competition assays were performed on LB agar plates using a 1:1 ratio of attacker to prey and incubating at 37°C for 5 hours. Attacker strains were *P. aeruginosa* and prey strains were either *P. putida* harboring pRL662-*gfp* or *P. aeruginosa* strains with pBK-miniTn7-gfp2 integrated. Competitions were recovered and serially diluted prior to spot plating on LB agar plates with or without antibiotics for selection and growing overnight at 30°C. Survival was assessed by quantitative colony counts on selective media (using gentamicin or rifampicin) or by measuring GFP fluorescence levels of the obtained cells after overnight growth and resuspension in PBS using a Fluostar Omega plate reader (BMG Labtech).

SDS-PAGE and western blot analysis. Samples were loaded on 12% SDS-PAGE gels and electrophoresis was performed at 120V. The proteins were then transferred onto an Amersham Protran nitrocellulose membrane 0.2 µm (GE Healthcare) using a Trans-blot SD semi-dry transfer cell (BioRad). The nitrocellulose membrane was blocked with PBST 5% milk, incubated with the appropriate primary antibody (V5 (Invitrogen), 1:5000 dilution; HA (Biolegend), 1:10000 dilution; MBP-HRP (Abcam),1:1000 dilution; Flag 1:20000 (Sigma); VgrG1b, 1:500 dilution; TssB1, 1:1000 dilution; TssB2, 1:1000 dilution; , Hcp1, 1:500 dilution; RNAP, 1:1000 dilution) and secondary antibody (mouse anti-rabbit HRP-conjugated (Sigma), 1:5000 dilution) separately and developed with Super Signal West Pico Chemiluminescent Substrate (Thermo Scientific) or Luminata Forte Western HRP substrate (Millipore) using a Fuji Imager LAS 3000.

Dot Blots. For Tse7-Tsi7 interactions purified MBP-Tse7, MBP-EspJ and TssB1C1 were spotted on nitrocellulose membrane. The membrane was blocked with PBST 5% milk for 1 hour. *E. coli* DH5a overexpressing Tsi7-HA^{PAK} was resuspended in 100 mM NaCl, 20 mM Tris, 10% glycerol, 0.5 mM EDTA 2% skim milk powder and 1 mM DTT (pH 7.6) and sonicated. Sonicated lysates were applied to the membrane and incubated overnight at 4°C. For Tse7-VgrG1b interactions, purified MBP-Tse7 and MBP-EspJ were spotted on nitrocellulose membrane. Membranes were blocked with PBST 5% milk and 2.5% bovine serum albumin for 7 hours. *E. coli* DH5a overexpressing VgrG1b-Flag^{PAK}, VgrG2b-Flag^{PAK}

or Hcp1-Flag^{PAK} were resuspendend in 100 mM NaCl, 20 mM Tris, 10% glycerol, 2% skim milk powder and 0.1% Tween-20 (pH 7.6) and sonicated. Lysates were applied to the membranes and incubated overnight at room temperature. The membranes were immunoblotted as described above.

Microscopy. For fluorescence microscopy of DAPI-strained cells, *E. coli* BL21 harboring pET28a-based plasmids were grown and induced. At OD_{600} 1, cells were harvested and resuspended in 100 µl of 1xPBS. Suspensions were incubated with 0.4 µl/ml DAPI for 30 min. One µl of the cell suspension was added to a 35 mm µDish, high glass bottom (Ibidi) which was then covered with a 1% agarose pad in 1x PBS and was visualized with an Axio Observer Z1 Fluorescence microscope.

Galleria mellonella infection assay. *G. mellonella* assays were performed as previously described (5). Briefly, overnight cultures were sub-cultured to OD_{600} 0.1 and grown in TSB at 37°C until OD_{600} 0.8-0.9. Cells were then pelleted, washed three times in sterile PBS, fixed to OD_{600} 1 and serially diluted to 10^{-8}. Infections were performed with 10 µl containing approximately 15 bacteria in PBS or PBS alone as a negative control. Suspensions were injected using a Hamilton syringe into the front right proleg of each *Galleria*. *Galleria* were subsequently placed at 4°C until all injections were performed for each experiment and then transferred to a 37°C incubator. The order of infection was rotated between the individual experiments. The *Galleria* were monitored on an hourly basis for unresponsiveness and death. Inocula were enumerated for each experiment.

Bioinformatics analyses. Bioinformatic analyses were performed using Interproscan, pBlast, Jalview (for protein sequence alignments), ACT (for genome comparison) and Phyre2 (6–10) (for protein structure prediction). The figures for the cluster alignments were created using Easyfig (11). Modeling of protein structures was performed using Phyre2 and PyMOL (The PyMOL Molecular Graphics System, Version 1.8 Schrödinger, LLC). Tse7 and VgrG1b trimer Phyre 2-predicted structures were modelled onto VrgG1a (PDB code: 4MTK) and VCA0105 (PDB code: 4JIV). Phylogenic trees were constructed using the MEGA6 software (Test: Interior-branch test, Number of Bootstrap: 150, Method: Jones-Taylor-Thornton model) (12, 13). The representative *P. aeruginosa* genomes analyzed were *P. aeruginosa*: 19BR Accession Number: AFXJ01000001, 213BR Accession Number: NC_002516, B136-33 Accession Number: NC_020912, DK2 Accession Number: CP003149, LES431 Accession Number: NC_023066, LESB58 Accession Number: FM209186.1, LESlike1 Accession Number: CP006984.1, M18 Accession Number: NC_017548, MTB1 Accession Number: CP006853, PA1 Accession Number: CP004054, PA1R Accession Number: NC_022806.1, PA7 Accession Number: NC_009656, UCBPP-PA14 Accession Number: NC_008463, PA96 Accession Number: CP007224, PAK laboratory strain, PAO1 Accession Number: NC_002516, RP73 Accession Number: NC_021577, SCV20265 Accession Number: CP006931, YL84 Accession Number: NZ_CP007147.

Statistical analysis. Statistical analysis was performed using GraphPad Prism version 5 or 6.01 for Windows, GraphPad Software, (La Jolla California USA). Flow cytometry experiments were analyzed using ordinary two-way ANOVA with Sidak's multiple comparisons test. Competition assays were analyzed using ordinary one-way ANOVA with Dunnett's or Tukey's multiple comparisons test. Survival of *G. mellonella* infected with PAK strains was plotted on a Kaplan-Meier survival analysis plot and a Log-rank Mantel-Cox test was performed.

SUPPLEMENTARY INFORMATION FIGURES

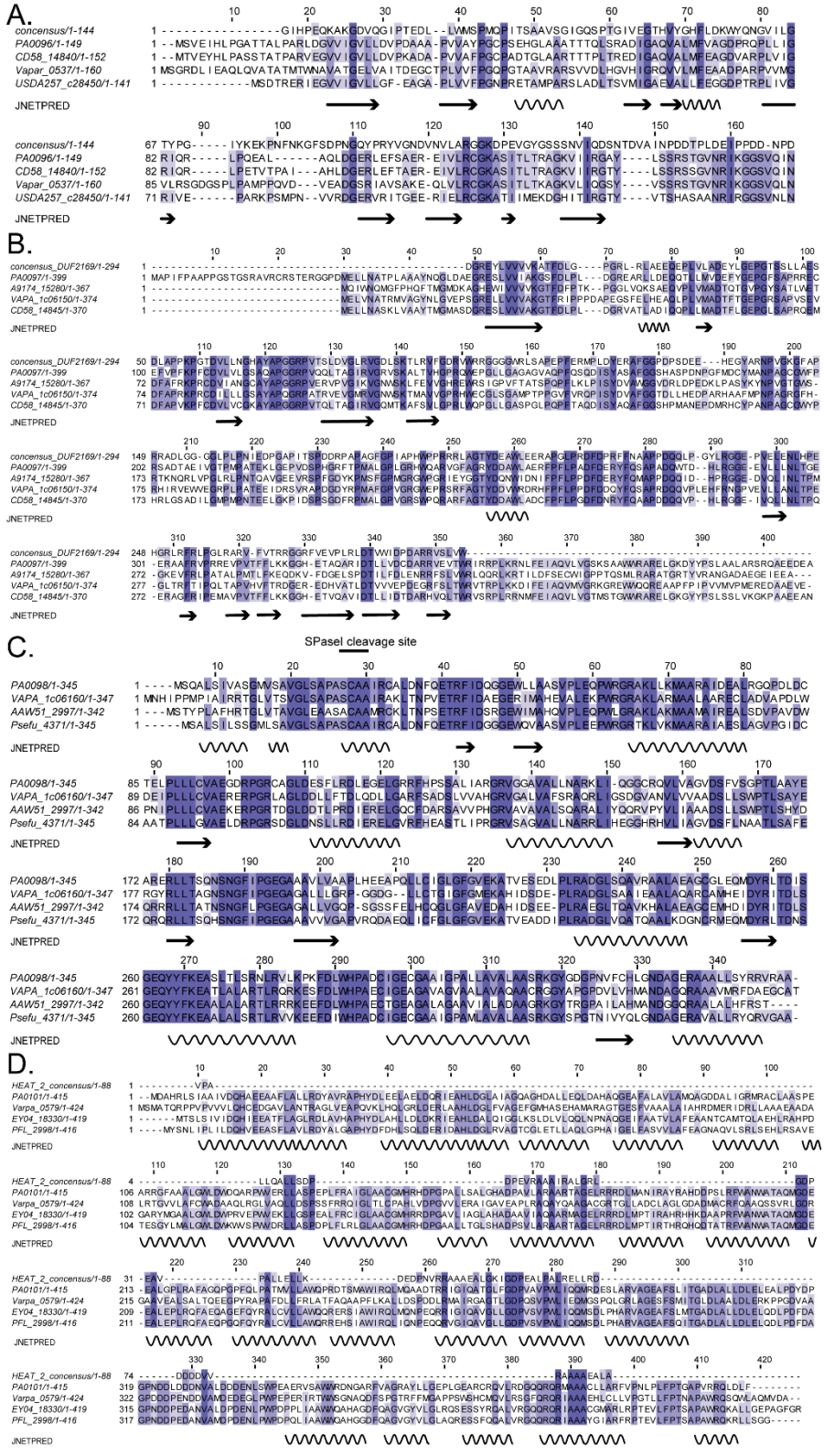

Fig. S1. Protein sequence alignments of PA0096, PA0097, PA0098, PA0101 and predicted secondary structure. (*A*) Alignment of PA0096 homologues with a Gp5_OB fold consensus. Homologues from the following bacteria were used: *P. aeruginosa* PAO1, *Pseudomonas brassicacearum* DF41, *Variovorax paradoxus* S110, *Sinorhizobium fredii*

USDA 257. (*B*) Alignment of PA0097 homologues with a DUF2169 consensus. Homologues from the following bacteria were used: *P. aeruginosa* PAO1, *Mesorhizobium loti* NZP2037, *Variovorax paradoxus* B4, *Pseudomonas brassicacearum* DF41. (*C*) Alignment of PA0098 homologues. Homologues from the following bacteria were used: *P. aeruginosa* PAO1, *Variovorax paradoxus* B4, *Polyangium brachysporum*, *Pseudomonas fulva*. The SPaseI signal peptide cleavage site is also indicated. (*D*) Alignment of PA0101 homologues with a HEAT_2 consensus. Homologues from the following bacteria were used: *P. aeruginosa* PAO1, *Variovorax paradoxus* EPS, *Pseudomonas chlororaphis* PA23, *Pseudomonas protegens* Pf-5. All alignments were performed using Muscle (12). JetNet secondary structure predictions are illustrated with arrows (β-sheets) and curvy lines (α-helices) (14).

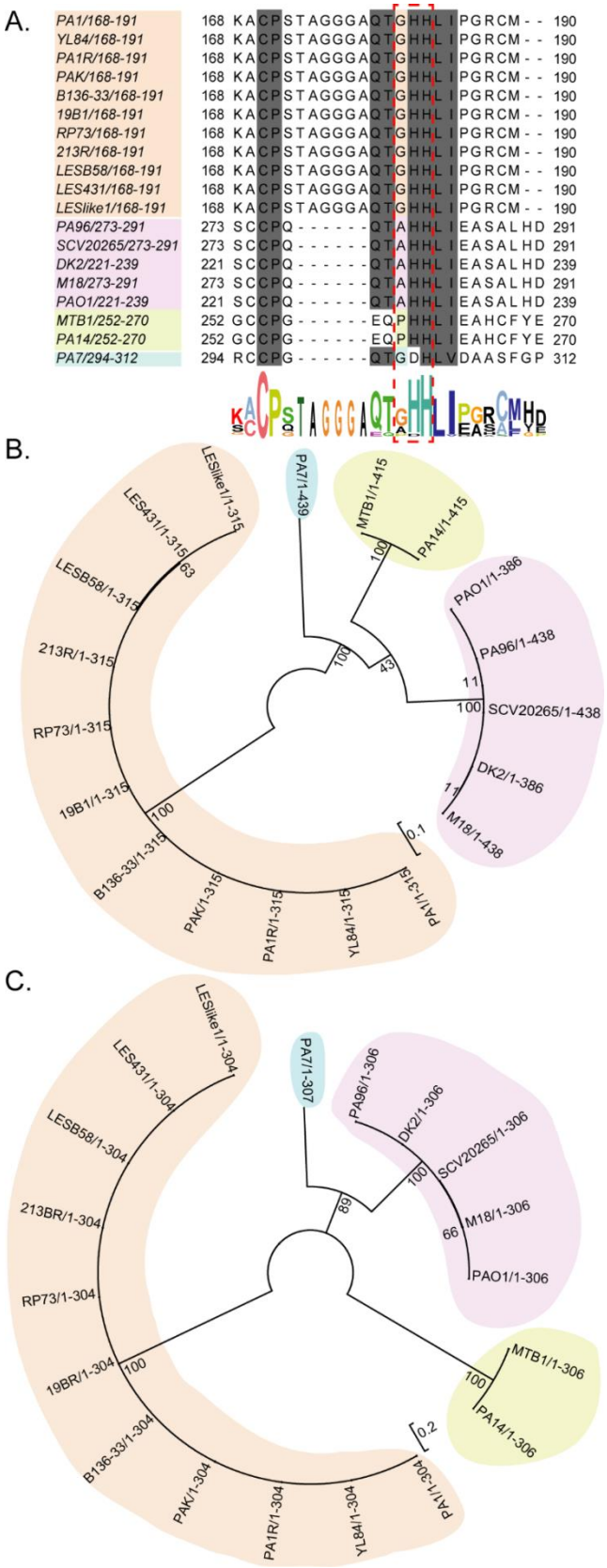

Fig. S2. Divergent Tse7 and Tsi7 pairs are found in different *P. aeruginosa* strains. (*A*) Tse7 contains a C-terminal Tox-GHH2 putative nuclease catalytic site (red dashed box) which varies between *P. aeruginosa* strains. The sequence alignment was performed with Muscle (15). Grey-shaded amino acids indicate highly-conserved residues. The shading on

the strain annotations illustrates the phylogenetic clades of Tse7 (see also phylogenetic tree in panel *(B)*) which also feature corresponding differences in their catalytic-site residues (shaded amino acids within the red dashed box). The Modified Weblogo3 under the sequence alignment depicts the conservation of the residues of the catalytic site region. (*B*) Tse7 homologues from *P. aeruginosa* clade into four groups as indicated by the different color shading. The tree with the highest log likelihood (-2266.3644) is shown, drawn to scale, and branch lengths are measured using the number of substitutions per site (total = 291). (*C*) Tsi7 homologues from *P. aeruginosa* clade into four groups as indicated by the different color shading. The tree with the highest log likelihood (-2282.4040) is shown, drawn to scale, with branch lengths measured using the number of substitutions per site (total = 233). Initial trees for the heuristic search were obtained automatically by applying Neighbor-Join and BioNJ algorithms to a matrix of pairwise distances estimated using a JTT model, and then selecting the topology with superior log likelihood value (12). All positions containing gaps and missing data were eliminated. Evolutionary analyses were conducted in MEGA6 (13).

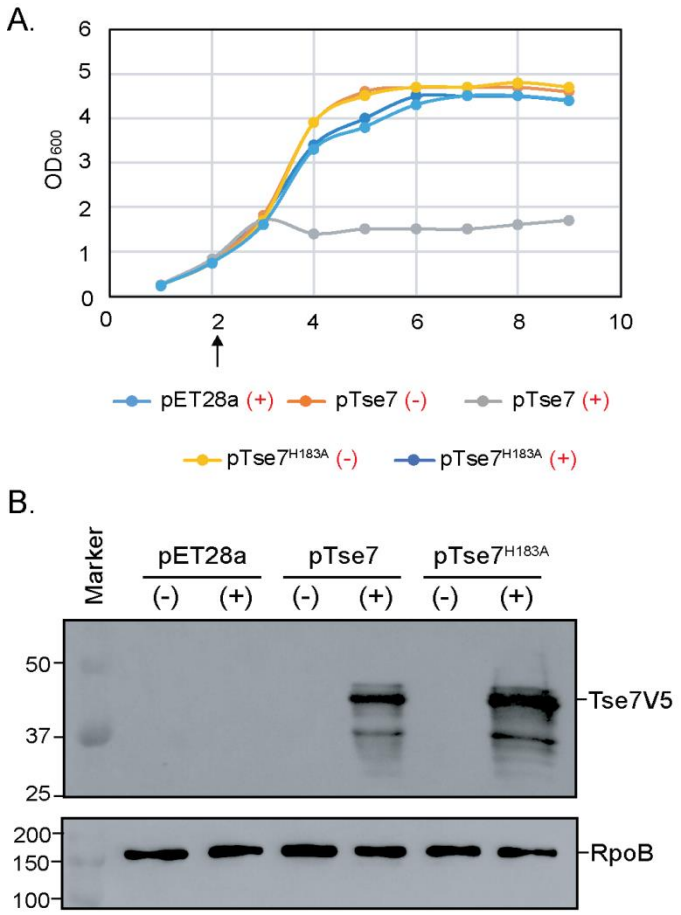

Fig. S3. Tse7 is toxic to *E. coli*. (*A*) Growth curves of *E. coli* BL21 pLysS cells harboring pET28a, pTse7 or pTse7^{H183A} grown in the absence of antibiotic selection. The arrow indicates the time of induction with 0.5 mM IPTG. Expression of Tse7 compromises growth (grey curve) whilst expression of Tse7^{H183A} does not (blue curve). (*B*) Western blot analysis using an anti-V5 antibody demonstrates that both V5-tagged Tse7 and Tse7^{H183A} are expressed. RpoB is used as a loading control. Samples for western blot analysis were recovered from the cultures used for panel *(A)* at 4 hours post-induction. Symbols (+) and (-) indicate the addition or not of IPTG, respectively. The predicted size of Tse7V5 is 39.3 kDa.

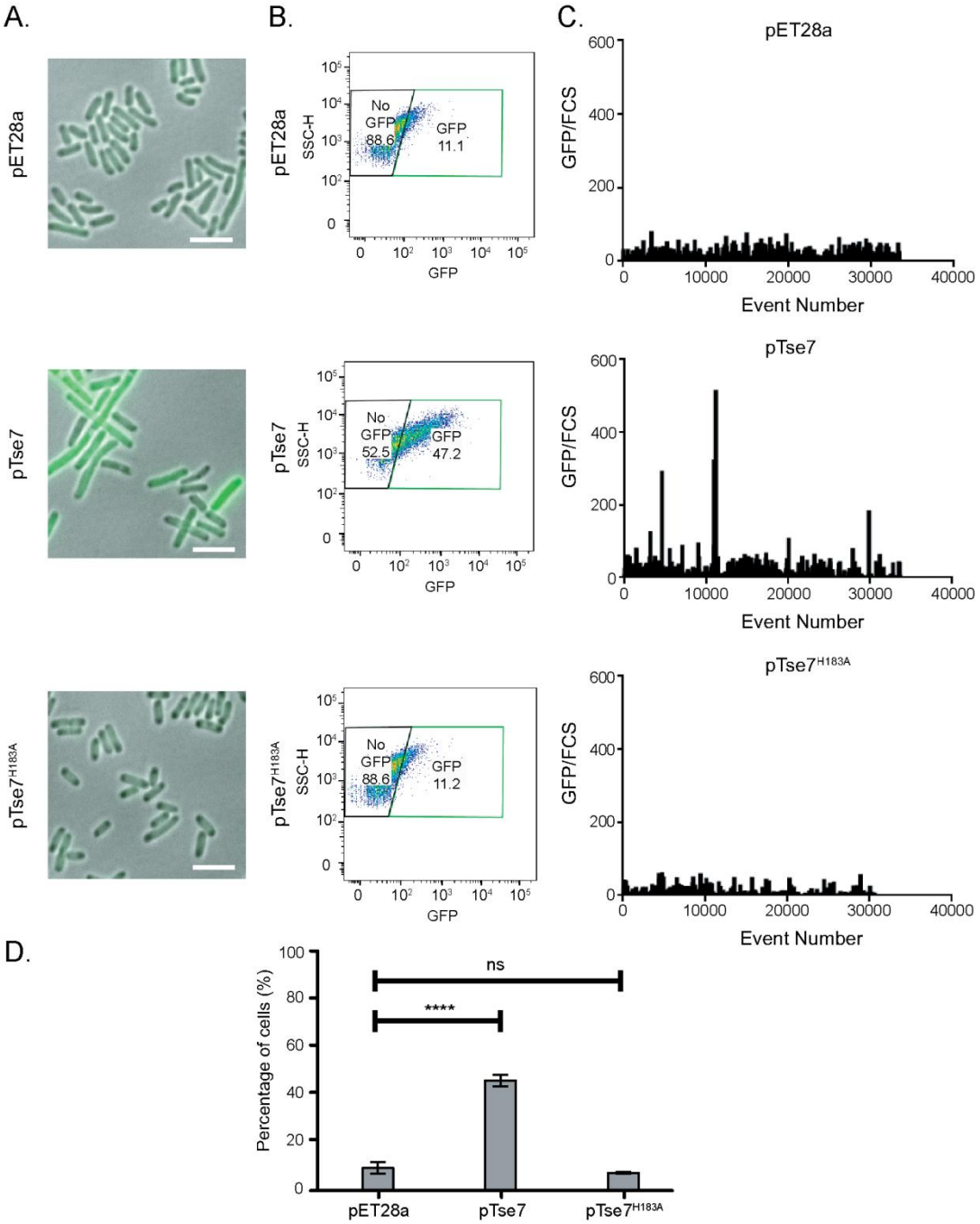

Fig. S4. Expression of Tse7 leads to induction of the SOS response. (*A*) Fluorescence microscopy of *E. coli* BL21 cells harboring pET28a, pTse7 or pTse7H183A after 2 hours of induction with 0.5 mM IPTG, in the presence of the SOS reporter pP*recA-gfp*. Enhanced expression of the stable superfolder GFP is observed after expression of Tse7 but not Tse7^{H183A} suggesting that DNA damage is occurring with the native toxin but not with the catalytic-site variant. Scale bars are at 6 µm. (*B*) Flow cytometry analysis demonstrating expression of Tse7 results in an increase in GFP-positive cells, indicating the induction of the SOS response (through the pP*recA-gfp* reporter). Enhanced expression of the SOS reporter was not observed in cells harboring pET28a or pTse7^{H183A}. (*C*) Graphs depicting the GFP signal relative to the forward scatter (as a measure of the cell length) plotted against the number of events. (*D*) Quantification of (*B*), the graph depicts the average of three

independent flow cytometry experiments ±SD; statistical significance is indicated (**** equals $P \leq 0.0001$) two-way ANOVA Sidak's multiple comparisons test.

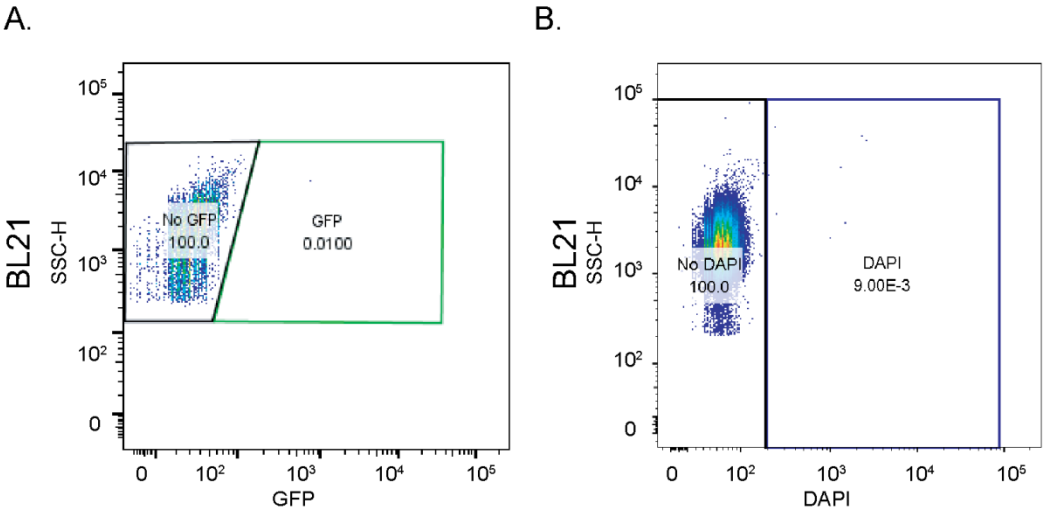

Fig. S5. Flow cytometry of control samples for Fig. S4 and Fig. 3. (*A*) *E. coli* BL21 cells with no pP*recA-gfp* do not exhibit any GFP fluorescence. (*B*) *E. coli* BL21 with no DAPI stain added do not exhibit any DNA staining.

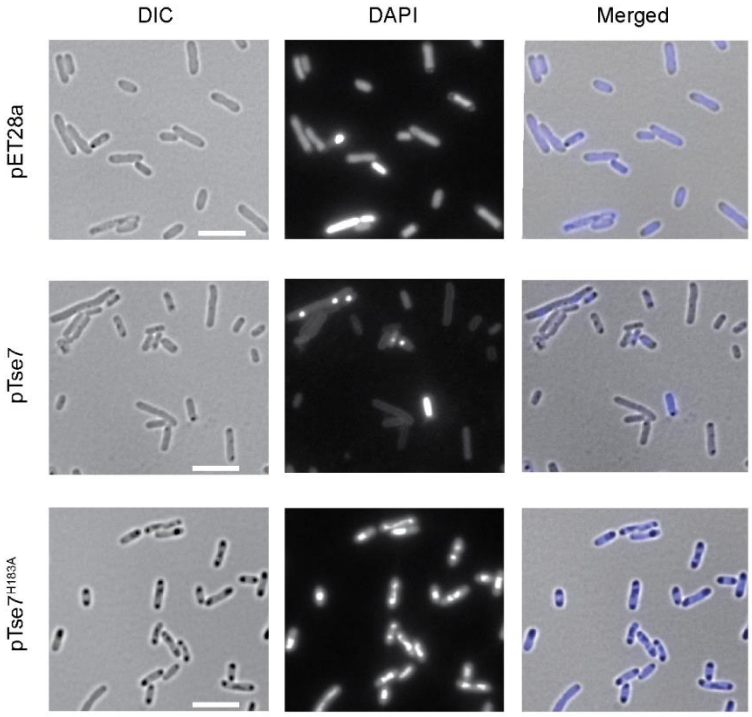

Fig. S6. Expression of Tse7 leads to degradation of DNA. The figure shows the separate channels (DIC and DAPI) for the microscopy experiments presented in Fig. 3*A* on cultures expressing pET28a, Tse7 and Tse7^{H183A}. The darker intensities at the pole visible in the DIC are likely inclusion bodies of the overexpressed protein. Clear loss of DAPI staining is visible for cells expressing Tse7.

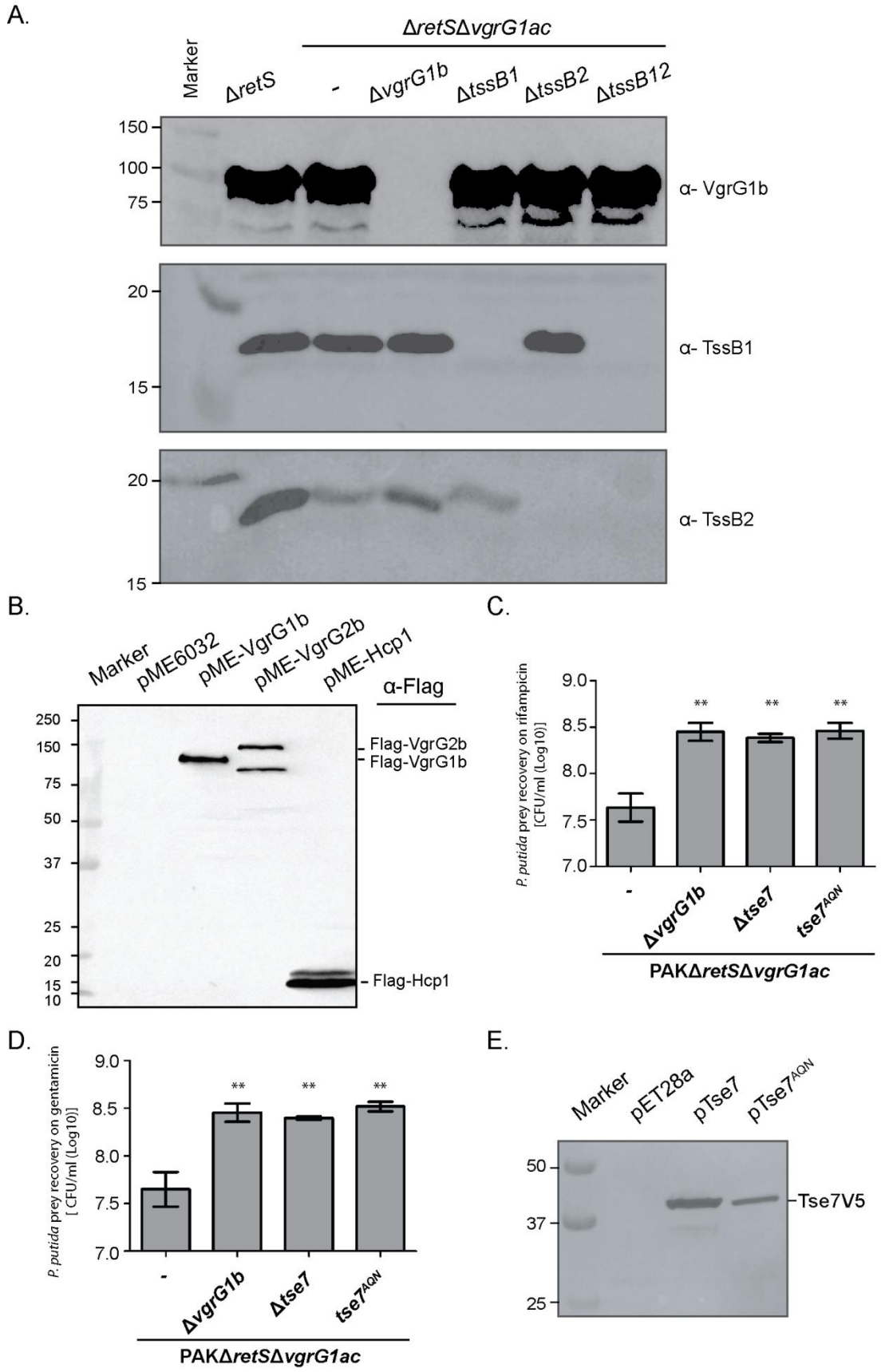

Fig. S7. Western blot controls for Fig. 4 and 5 and complementary competition experiments for Fig. 5. (*A*) Western blots analysis on whole cell lysates from *P. aeruginosa*

PAK wild-type and derivative strains used in the competition assays with *P. putida* shown in Fig. 4. This analysis confirms the appropriate gene deletion in the strains used. Antibodies against VgrG1b (top panel), TssB1 (middle panel) and TssB2 (bottom panel) (expected sizes: 82.8, 18.9 and 18.3 kDa) were used. (*B*) Western blot analysis using an anti-Flag antibody, to confirm the expression of VgrG1b, VgrG2b and Hcp1 (expected sizes: 83.7, 114 and 18.4 kDa) from pME-derivative constructs expressed in *E. coli.* (*C*, *D*) Quantification of bacterial competition assays showing loss of *P. putida* KT2440 killing when competing with a *tse7*^{AQN} mutant, as is the case for a *vgrG1b* or a *tse7* deletion mutant. Results are expressed as Log10 of *P. putida* KT2440 colony forming units after selection on (*C*) gentamicin (selection of pRL662-*gfp*) or on (*D*) rifampicin (selection of KT2440). The graphs depict the average of n=3 independent experiments ±SD; statistical significance indicated (** equals $P \leq 0.01$) one-way ANOVA Dunnett's multiple comparison test against the first column in each graph. (*E*) Western blot analysis using an anti-V5 antibody, confirming the expression and stability of Tse7 and Tse7^{AQN} (expected size: 39.3 kDa) from pET28a-derivative plasmids in *E. coli.*

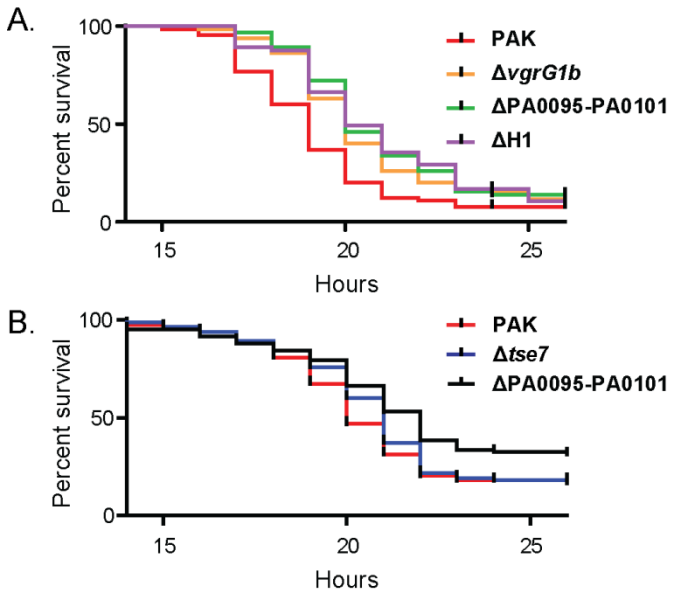

Fig. S8. Involvement of the *vgrG1b* cluster to T6SS virulence. (*A*) The *vgrG1b* cluster contributes to virulence. Kaplan-Meier survival analysis of *G. mellonella* infected with PAK, PAKΔ*vgrG1b*, PAKΔPA0095-PA0101 (deletion of the entire *vgrG1b* cluster) or PAKΔH1 (deletion of the H1-T6SS cluster). Results are from four independent experiments, n = 65 per strain, statistical analysis was performed, $P < 0.005$ (Log-rank Mantel-Cox test). (*B*) Tse7 is not contributing to the virulence observed in *G. mellonella* infection. Kaplan-Meier survival analysis of *G. mellonella* infected with PAK, PAKΔ*tse7*, PAKΔPA0095-PA0101. Results are from seven independent experiments, n = 83 per strain, statistical analysis was performed, $P < 0.05$ (Log-rank Mantel-Cox test).

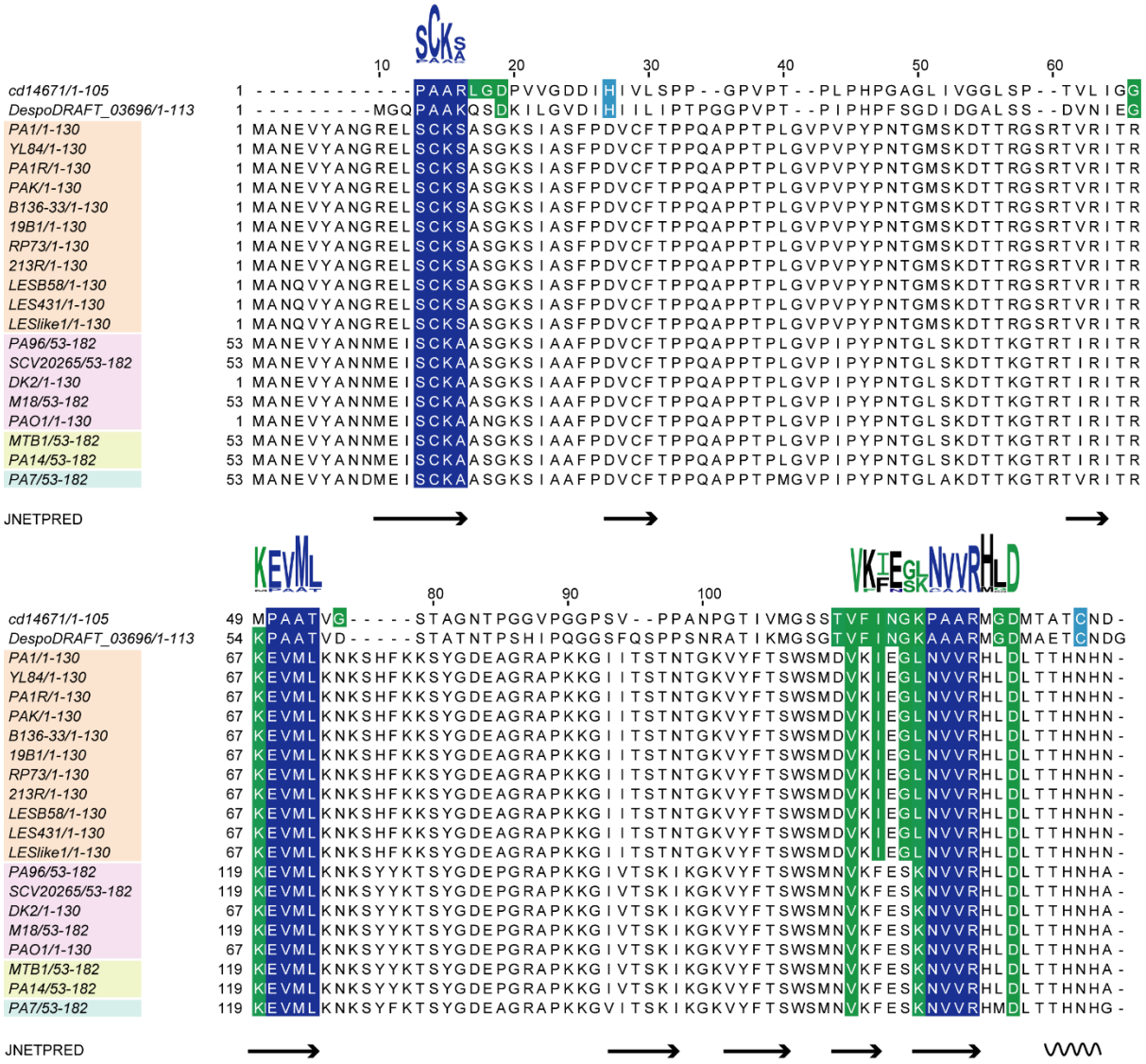

Fig. S9. Sequence alignment of the N-terminal PAAR-like domain of Tse7. The N-terminus of Tse7 from different *P. aeruginosa* strains was aligned with *DespoDRAFT_03696* and the consensus of DUF4150 cd14671 using Muscle (13). Blue shading indicates predicted PAAR-like motifs, while the residues typically observed next to PAAR motifs and the residues predicted to be involved in metal ion binding are highlighted in green and cyan, respectively.

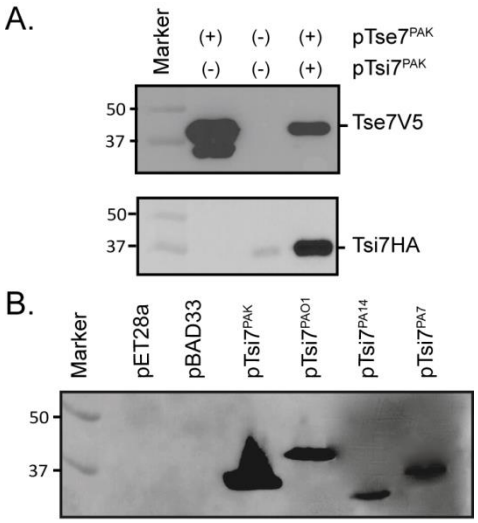

Fig. S10. Confirmation of expression of Tse7 and Tsi7. (*A*) Western blots analysis of whole cell extracts examined in Fig. 6*A* using an anti-V5 antibody for Tse7-V5 (expected size 39.3 kDa) and an anti-HA antibody for Tsi7-HA (expected size 34.6 kDa). Symbols (+) and (-) indicate addition or not of IPTG, respectively. (*B*) All Tsi7 variants are expressed. Western blot analysis of the whole cell extracts examined in Fig. 6*D* using an anti-HA antibody. Expected sizes: Tsi7^{PAK}, 39.3 kDa; Tsi7^{PAO1}, 34.9 kDa; Tsi7^{PA14}, 27.9 kDa; Tsi7^{PA7} and 35 kDa.

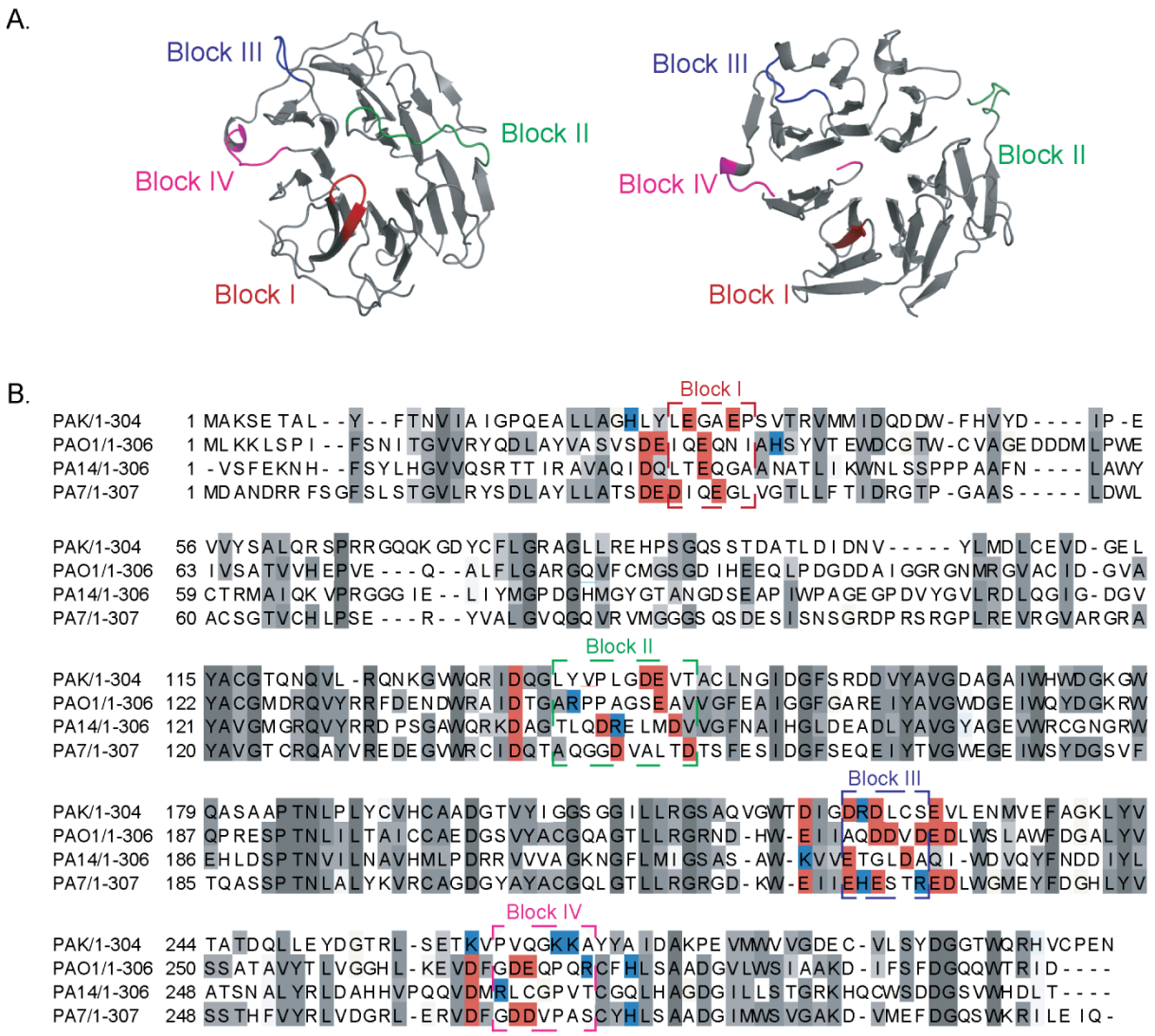

Fig. S11. Identification of putative interactions blocks between Tse7 and Tsi7. (*A*) Modelled structures of Tsi7^{PAK} (left panel) and Tsi7^{PA7} (right panel). Colored regions show the areas of interest (Blocks I-IV) which are predicted to mediate the interaction between Tsi7 and Tse7. (*B*) Sequence alignment of the Tsi7 immunity protein from common *P. aeruginosa* strains. Grey shading indicates conserved areas throughout the sequence. Negatively- and positively-charged residues in specific areas of interest are highlighted by red and blue shading, respectively. Areas of potential interaction of Tsi7 with Tse7 (named Blocks I-IV and marked with dashed boxes) were identified as sections of Tsi7 that are significantly different between the four strains, have high charge density, and are located on parts of the protein which are not structured. The sequence alignment was performed using Muscle (15).

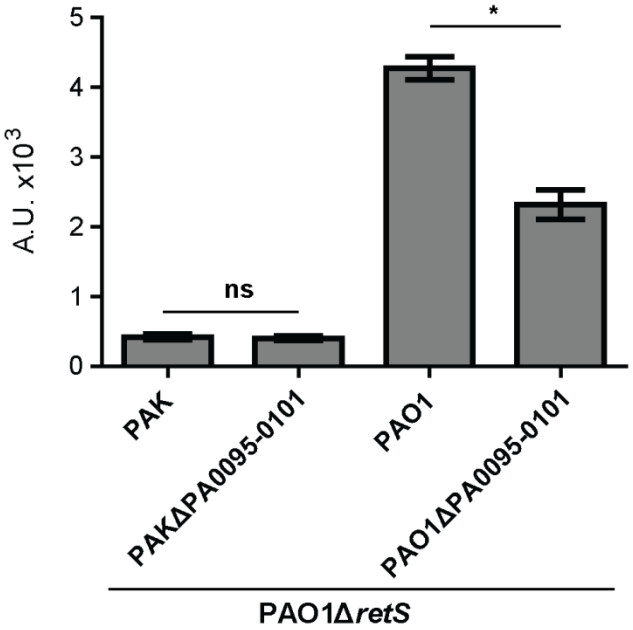

Fig. S12. The *tse7* gene and the *vgrG1b* cluster contribute to interbacterial competition. Quantification of a bacterial competition assay between *P. aeruginosa* PAO1Δ*retS* (attacker) and PAK or PAO1 or their mutants lacking the *vgrG1b* cluster (PAKΔPA0095-0101 or PAO1ΔPA0095-0101, respectively) with pBK-miniTn7-gfp2 integrated (preys). PAO1Δ*retS* is active for H1-T6SS-dependent killing. On the *y* axis, fluorescence measure indicates survival of the prey strains. Deletion of PA0095-0101, which includes *tsi7* (PA0100) renders PAO1 more susceptible to killing. Results are the average of n=3 independent experiments ±SD; statistical significance indicated (* equals $P \leq 0.05$) one-way ANOVA Tukey's multiple comparison test.

SUPPLEMENTARY INFORMATION TABLES

Table S1. Bioinformatic summary of the *vgrG1b* operon

Gene name	Predicted domains	Size (kDa)	Predicted structure	Phyre2 statistics
PA0095 *vgrG1b*	VgrG family Gp5 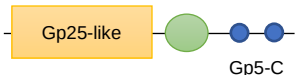	82.8	VgrG 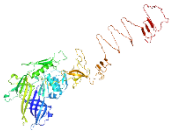	**Coverage:** 82% **Confidence:** 100%
PA0096	Partial Gp5 	15.6	OB-fold 	**Coverage:** 95% **Confidence:** 99.9%
PA0097	DUF2169 	43.6	Immunoglobulin-like	**Coverage:** 10% **Confidence:** 71.4%
PA0098	Thiolase-like 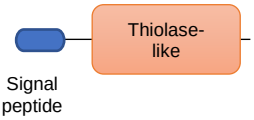	36.8	3-oxoacyl-[acyl-carrier-protein] 	**Coverage:** 99% **Confidence:** 100%
PA0099 (*tse7*)	DUF4150, Tox-GHH2 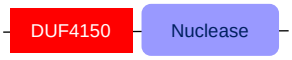	33.7	N-terminal PAAR 	**Coverage:** 20% **Confidence:** 97.3%
PA0100 (*tsi7*)	Calcium-dependent phosphotriesterase superfamily	33.4	7-bladed β-propeller 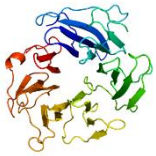	**Coverage:** 99.9% **Confidence:** 93%
PA0101	CHP02270 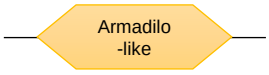	45.2	Heat repeat 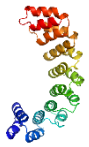	**Coverage:** 57% **Confidence:** 99.9%

Table S2. Schematic representation of the nuclease domains observed T6SS toxins

Predicted nuclease domains		T6SS depended nuclease
HNH superfamily	HNH endonuclease	RhsA — Rhs — HNH
		Tke2 — PAAR — Rhs — HNH
	AHH nuclease	VP1415 — DUF4150 — HNH
Pyocin/colicin DNase		Hcp_ET3 — Hcp — DNase
Toxin_43		Tde1 — HxxD
		Tde2 — DUF4150 — HxxD
NS_2		RhsB — Rhs — nuclease
Tox-REase1		Tke10 — MIX — nuclease

Table S3. Bacterial strains used in this study.

Strain name	Description	Source
Escherichia coli		
DH5α	*F-Φ80lacZΔM15Δ(lacZYA-argF) U169 recA1 endA1 hsdR17 (rK-,mK-) phoA supE44λ -thi-1 gyrA96 relA1*	Life Technologies
BL21 DE3	*B dcm ompT hsdS(rB-mB-) gal*	Life Technologies
BL21 DE3 pLysS	*B dcm ompT hsdS(rB-mB-) gal* pLysS*[T7p20 orip15A](CmR)*	Life Technologies
CC118 λpir	*phoA20 thi-1 rspE rpoB argE (Am) recA1*	Laboratory strain
SM10 λpir	*thi-1 thr leu tonA lacY supE recA*::RP4-2-Tc::Mu λ*pir*, KmR	(16)
Pseudomonas aeruginosa		
PAK	Wild-type prototroph	Laboratory strain
Δ*retS*	*retS* deletion	(17)
Δ*retS*Δ*vgrG1ac*	*retS*/*vgrG1a*/*vgrG1c* deletion	(17)
Δ*retS*Δ*vgrG1abc*	*retS*/*vgrG1a*/*vgrG1b*/*vgrG1c* deletion	(17)
Δ*retS*Δ*vgrG1ac*Δ*tssB1*	*retS*/*vgrG1a*/*vgrG1c*/*tssB1* deletion	This study
Δ*retS*Δ*vgrG1ac*Δ*tssB2*	*retS*/*vgrG1a*/*vgrG1c*/*tssB2* deletion	This study
Δ*retS*Δ*vgrG1ac*Δ*tssB12*	*retS*/*vgrG1a*/*vgrG1c*/*tssB1*/*tssB2* deletion	This study
Δ*retS*Δ*vgrG1ac*Δ*tse7*	*retS*/*vgrG1a*/*vgrG1c*/*tse7* deletion	This study
Δ*retS*Δ*vgrG1actse7*^{AQN}	*retS*/*vgrG1a*/*vgrG1c* deletion and T61A/ R63Q/ I64N point mutations on *tse7*	This study
Δ*retS*Δ*vgrG1actse7*^{H183A}	*retS*/*vgrG1a*/*vgrG1c* deletion and H183A point mutation on *tse7*	This study
ΔH1-T6SS	H1-T6SS cluster deletion (PA0071-PA0095)	(4)
Δ*vgrG1b*	*vgrG1b* deletion	This study
ΔPA0095-PA0101	*vgrG1b* cluster deletion (PA0095-PA0101)	This study
Δ*tse7*	*tse7* deletion	This study
tse7^{AQN}	T61A/ R63Q/ I64N point mutations on *tse7*	This study
pBK-miniTn7-gfp2	GFP-labelled wild type	This study
ΔPA0095-PA0101 pBK-miniTn7-gfp2	GFP-labelled *vgrG1b* cluster deletion	This study

Strain name	Description	Source
PAO1	Wild-type prototroph	Laboratory strain
pBK-miniTn7-gfp2	GFP-labelled wild type	This study
ΔPA0095-PA0101	*vgrG1b* cluster deletion (PA0095-PA101)	This study
ΔPA0095- PA0101 pBK-miniTn7-gfp2	GFP-labelled *vgrG1b* cluster deletion	This study
PA14	Wild-type prototroph	Laboratory strain
PA7	Wild-type prototroph	Laboratory strain
Pseudomonas putida		
KT2440R	Rf^R	Juan-Luis Ramos lab

Table S4. Oligonucleotide primers used in this study.

Primer name	DNA Sequence (5´-3´)
FW *tse7* (BamHI, pCR2.1 RBS)	GTACTGGATCCTTCACACAGGAAACAGCTATGGC CAACGAGGTCTATGCCAACGG
RV *tse7* (XhoI, V5)	AGTACCTCGAGCTACGTAGAATCGAGACCGAGGA GAGGGTTAGGGATAGGCTTACCTGGACGTCCCGC AGGTGCCG
FW *tsi7* (XbaI, pET RBS)	ATTAGTCTAGATAAGAAGGAGATATACATATGGC AAAGAGCGAGACCGCCCTCTAT
RV *tsi7* (HindIII, HA)	AAGTTAAGCTTTTAGCACGCGTAGTCCGGCACGTC GTACGGGTAGTTCTCCGGGCAGACATGACGCTGC CAGGT
FW *tse7* (NcoI)	GTACTCCATGGATGGCCAACGAGGTCTATGCCAA CGG
RV *tse7* (XbaI, V5)	AGTATCTAGACTACGTAGAATCGAGACCGAGGAG AGGGTTAGGGATAGGCTTACCTGGACGTCCCGCA GGTGCCG
FW *tse7* (BamHI)	GTACTGGATCCATGGCCAACGAGGTCTATGCCAA CGG
RV *tse7* (XbaI)	AGTACTCTAGACTATGGACGTCCCGCAGGTGCCG
FW *tse7*^{H183A}	CGCACAGACCGGCCACGCTCTGATTCCTGGTCGCT GTAT
RV *tse7*^{H183A}	GCATACAGCGACCAGGAATCAGAGCGTGGCCGGT CTGTG
tse7 T61A, R63Q, I64N P1	GCAGTACAAGACACCCGCAAGGAAGTGATG
tse7 T61A, R63Q, I64N P2	GTCTTGTACTGCCCGGCTACCTCGGGTG
tse7 T61A, R63Q, I64N P3	GTAGCCGGGCAGTACAAGAC
tse7 T61A, R63Q, I64N P4	GCGGGTGTCTTGTACTGC
FW PA0100 (EcoRI, pET RBS)	GTTAAGAATTCTAAGAAGGAGATATACATATGGC AAAGAGCGAGACCGCCCTCTAT
RV PA0100 (XbaI, HA)	AAGTTTCTAGATTAGCACGCGTAGTCCGGCACGTC GTACGGGTAGTTCTCCGGGCAGACATGACGCTGC CAGGT
FW PA0100 PAO1 (XbaI, pET RBS)	ATTAGTCTAGATAAGAAGGAGATATACATATGTT GAAGAAACTCTCGCCGAT
RV PA0100 PAO1 (HindIII, HA)	AAGTTAAGCTTTTAGCACGCGTAGTCCGGCACGTC GTACGGGTAATCTATGCGCGTCCATTGCT
FW PA0100 PA14 (XbaI, pET RBS)	ATTAGTCTAGATAAGAAGGAGATATACATGTGTC GTTCGAGAAAAATCATTTC
RV PA0100 PA14 (HindIII, HA)	AAGTTAAGCTTTTAGCACGCGTAGTCCGGCACGTC GTACGGGTAGGTGAGGTCATGCCAGA
FW PA0100 PA7 (XbaI, pET RBS)	ATTAGTCTAGATAAGAAGGAGATATACATATGGA TGCGAATGACCGCC
RV PA0100 PA7 (HindIII, HA)	AAGTTAAGCTTTTAGCACGCGTAGTCCGGCACGTC GTACGGGTACTGAATCTCGAGAATCCGCTTCC
tssB2 P1	GCGCGGGATCCGGATCAGCGTCCATGTCATG
tssB2 P2	TCAGGCGTCTTTGGCCATGGCTTTTTC
tssB2 P3	ATGGCCAAAGACGCCTGAGCCACCCCT

tssB2 P4	GCGCGGGGCCCTGGAGACGTATTGCATCAGC
tssB2 P5	CAGGCGATGCGGGAAGTCGAAA
tssB2 P6	TCTGCCACTTGGCGAACTGC
tssB1 P1	ATGCCCTGGCCATCGAGAG
tssB1 P2	TTACGCCTGGCTTCCCATCTTGTTTCTCCC
tssB1 P3	ATGGGAAGCCAGGCGTAAGAGGATTCC
tssB1 P4	GGCGACTGGTCGAAGTAGTAGT
tssB1 P5	CGACCCCACCTTCCGTATCAAC
tssB1 P6	CGATGTAGCGGGAGTCCTCG
Tse7 P1	AGTCGATTCCTACCTGACCG
Tse7 P2	CTATGGACGGTTGGCCATCTAGTTCGC
Tse7 P3	ATGGCCAACCGTCCATAGGAACTGAAC
Tse7 P4	AGTAGAGCGGCAGGTTGG
Tse7 P5	CAATTGGTGGGGATGGCTG
Tse7 P6	AAGCCTTCTTACCCTGCACT
vgrG1b P1	TACCTGGCGCAGCATCAGGTC
vgrG1b P2	TCAGTTCTGAAGTGCCATGAAATCATC
vgrG1b P3	ATGGCACTTCAGAACTGAAGCGGCGC
vgrG1b P4	GTCGAGCCCCTGGTTGTAGG
vgrG1b P5	TTCTCGGCGTTTTCCAGTTG
vgrG1b P6	GGCGTTCAACAGTTCCATGT
Cluster mutant P1	CACTGGTAGTCGAGGAGCAC
Cluster mutant P2	TTCGTCGAATCCTTGATCCACGTCCATCA
Cluster mutant P3	GATCAAGGATTCGACGAATTTCCCTGCAC
Cluster mutant P4	GGGGAACTCTGGGTGATCA
Cluster mutant P5	CAGGGTCTGCATCGCCTG
Cluster mutant P6	ACCGTTCATCTGCCCGTAG
FW P*recA* (BamHI)	ATTAGGATCCAAACCGGTGGGCACTGTGT
RV P*recA* (HindIII)	ATCAGAAGCTTTGAAATCCTCACGTGTTCGACTTG
*vgrG1b*_flag_F	CGGAATTCATGGCACTTGCGCAACAGACCCGCCT GGTC
*vgrG1b*_flag_R	GCCATGGCTATTTATCGTCGTCATCTTTGTAGTCGT TCTGGAGGATCTTGCG
*vgrG2b*_flag_F	CGGAATTCATGCGTCAAAGGGACCTGAAATTCAC CTTCG
*vgrG2b*_flag_R	GAGATCTCTATTTATCGTCGTCATCTTTGTAGTCGT ATCCCGTTGGGAAG
*hcp1*_flag_F	CGGAGCTCATGGCTGTTGATATGTTCATCAAGATC GGCGAC
*hcp1*_flag_R	GAGATCTCTATTTATCGTCGTCATCTTTGTAGTCG GCCTGCACGTTCTGGCG
*tssA2*_F	GGAATCCACTGTTGTCTGCCTTAT
*tssA2*_R	CCCTCTTTGGGAATTTTCCTATTC

Table S5. Plasmids used in this study.

Name	Description	Source
pET28a	Expression vector, Kan^R, IPTG inducible	Novagen
pTse7	pET28a with *tse7*-$V5^{PAK}$ cloned into BamHI/XhoI	This study
$pTse^{H183A}$	pTse7 harboring the H183A mutation	This study
pBAD33	Arabinose inducible vector, Cam^R	(18)
$pTsi7^{PAK}$	pBAD33 with *tsi7*-HA^{PAK} cloned into XbaI/HindIII	This study
$pTsi7^{PAO1}$	pBAD33 with *tsi7*-HA^{PAO1} cloned into XbaI/HindIII	This study
$pTsi7^{PA14}$	pBAD33 with *tsi7*-HA^{PA14} cloned into XbaI/HindIII	This study
$pTsi7^{PA7}$	pBAD33 with *tsi7*-HA^{PA7} cloned into XbaI/HindIII	This study
pRL662	Broad host range vector derived from pBBR1MCS-2 (19), Gm^R	Erh-Min Lai lab
pRL662-*gfp*	pRL662 expressing *gfp*, $Gent^R$	Erh-Min Lai lab
pMALxE	pMAL-c2x (New England Biolabs) derivative expression vector, Amp^R, IPTG inducible	(20)
pMALxE-$tse7^{H183A}$	pMALxE with *tse7* harboring the H183A mutation cloned into BamHI/XbaI	This study
pKNG101	Suicide vector, Sm^R	(21)
pKNG-*tssB1* mutator	pKNG101 with the mutator for the deletion of *tssB1*	(3)
pKNG-*tssB2* mutator	pKNG101 with the mutator for the deletion of *tssB2*	(3)
pKNG-*tse7*	pKNG101 with the mutator for the deletion of *tse7*	(4)
pKNG-$tse7^{AQN}$ mutator	pKNG101 with the mutator for point mutations T61A/R63Q/I64N in $tse7^{PAK}$	This study
pKNG-$tse7^{H183A}$ mutator	pKNG101 with the mutator for point mutation H183A in $tse7^{PAK}$	This study
pKNG-*vgrG1b*	pKNG101 with the mutator for the deletion of *vgrG1b*	(17)
pKNG-PA0096-PA0101	pKNG101 with the mutator for the deletion of PA0096-PA0101 in a PA0095 mutant	This study
pPROBE-TT´	Promoter-probe vector for construction of transcriptional fusions to *gfp*, Tet^R	(22) Urs Jenal lab
pP*recAgfp*	pPROBE-TT´ with the *recA* promoter from *P. putida* KT2440R driving expression of *gfp*	This study
pME6032	Broad host range expression vector, IPTG induction, Tet^R	(23)
pME-VgrG1b-Flag	pME6032 with *vgrG1b* (PA0095) amplified with a Flag tag and cloned into MCS	This study
pME-VgrG2b-Flag	pME6032 with *vgrG2b* (PA0262) amplified with a Flag tag and cloned into MCS	This study
pME-Hcp1-Flag	pME6032 with *hcp1* (PA0085) amplified with a Flag tag and cloned into MCS	This study
pBK-miniTn7-gfp2	For stable integration of gfp marker gene at neutral chromosomal site, Gm^R	(24)
pUX-BF13	Helper plasmid Tn7 transposition in trans, Amp^R	(25)

pCR-BluntII-TOPO	Sub-cloning vector, Kan^R	Life Technologies

REFERENCES

1. Vasseur P, Vallet-Gely I, Soscia C, Genin S, Filloux A (2005) The *pel* genes of the *Pseudomonas aeruginosa* PAK strain are involved at early and late stages of biofilm formation. *Microbiology* 151(3):985–997.

2. Gay P, Le Coq D, Steinmetz M, Berkelman T, Kado CI (1985) Positive selection procedure for entrapment of insertion sequence elements in gram-negative bacteria. *J Bacteriol* 164(2):918–21.

3. Allsopp LP, et al. (2017) RsmA and AmrZ orchestrate the assembly of all three type VI secretion systems in *Pseudomonas aeruginosa*. *Proc Natl Acad Sci U S A* 114(29):7707–7712.

4. Hachani A, Allsopp LP, Oduko Y, Filloux A (2014) The VgrG Proteins Are "à la Carte" Delivery Systems for Bacterial Type VI Effectors. *J Biol Chem* 289(25):17872–84.

5. McCarthy RR, et al. (2017) Cyclic-di-GMP regulates lipopolysaccharide modification and contributes to *Pseudomonas aeruginosa* immune evasion. *Nat Microbiol* 2(6):17027.

6. Jones P, et al. (2014) InterProScan 5: genome-scale protein function classification. *Bioinformatics* 30(9):1236–1240.

7. Waterhouse AM, Procter JB, Martin DMA, Clamp M, Barton GJ (2009) Jalview Version 2--a multiple sequence alignment editor and analysis workbench. *Bioinformatics* 25(9):1189–91.

8. Kelley LA, Mezulis S, Yates CM, Wass MN, Sternberg MJE (2015) The Phyre2 web portal for protein modeling, prediction and analysis. *Nat Protoc* 10(6):845–858.

9. Carver TJ, et al. (2005) ACT: the Artemis Comparison Tool. *Bioinformatics* 21(16):3422–3.

10. Boratyn GM, et al. (2013) BLAST: a more efficient report with usability improvements. *Nucleic Acids Res* 41(W1):W29–W33.

11. Sullivan MJ, Petty NK, Beatson SA (2011) Easyfig: a genome comparison visualizer. *Bioinformatics* 27(7):1009–1010.

12. Jones DT, Taylor WR, Thornton JM (1992) The rapid generation of mutation data matrices from protein sequences. *Comput Appl Biosci* 8(3):275–82.

13. Tamura K, Stecher G, Peterson D, Filipski A, Kumar S (2013) MEGA6: Molecular evolutionary genetics analysis version 6.0. *Mol Biol Evol* 30(12):2725–2729.

14. Cuff JA, Barton GJ (2000) Application of multiple sequence alignment profiles to improve protein secondary structure prediction. *Proteins* 40(3):502–11.

15. Edgar RC (2004) MUSCLE: multiple sequence alignment with high accuracy and high throughput. *Nucleic Acids Res* 32(5):1792–7.

16. de Lorenzo V, Timmis KN (1994) Analysis and construction of stable phenotypes in gram-negative bacteria with Tn5- and Tn10-derived minitransposons. *Methods Enzymol* 235:386–405.

17. Hachani A, et al. (2011) Type VI secretion system in *Pseudomonas aeruginosa*: secretion and multimerization of VgrG proteins. *J Biol Chem* 286(14):12317–27.

18. Guzman LM, Belin D, Carson MJ, Beckwith J (1995) Tight regulation, modulation, and high-level expression by vectors containing the arabinose PBAD promoter. *J Bacteriol* 177(14):4121–30.

19. Kovach ME, et al. (1995) Four new derivatives of the broad-host-range cloning vector pBBR1MCS, carrying different antibiotic-resistance cassettes. *Gene* 166(1):175–176.

20. Moon AF, Mueller G a, Zhong X, Pedersen LC (2010) A synergistic approach to protein crystallization: combination of a fixed-arm carrier with surface entropy reduction. *Protein Sci* 19(5):901–13.

21. Kaniga K, Delor I, Cornelis GR (1991) A wide-host-range suicide vector for improving reverse genetics in gram-negative bacteria: inactivation of the *blaA* gene of *Yersinia enterocolitica*. *Gene* 109(1):137–41.

22. Miller WG, Leveau JHJ, Lindow SE (2000) Improved *gfp* and *inaZ* Broad-Host-Range Promoter-Probe Vectors. *Mol Plant-Microbe Interact* 13(11):1243–1250.

23. Heeb S, Blumer C, Haas D (2002) Regulatory RNA as mediator in GacA/RsmA-dependent global control of exoproduct formation in *Pseudomonas fluorescens* CHA0. *J Bacteriol* 184(4):1046–56.

24. Koch B, Jensen LE, Nybroe O (2001) A panel of Tn7-based vectors for insertion of the gfp marker gene or for delivery of cloned DNA into Gram-negative bacteria at a neutral chromosomal site. *J Microbiol Methods* 45(3):187–95.

25. Bao Y, Lies DP, Fu H, Roberts GP (1991) An improved Tn7-based system for the single-copy insertion of cloned genes into chromosomes of gram-negative bacteria. *Gene* 109(1):167–8.